



University of Dundee

Chitin-Binding Protein of *Verticillium nonalfalfae* Disguises Fungus from Plant Chitinases and Suppresses Chitin-Triggered Host Immunity

Volk, Helena; Marton, Kristina; Flajsman, Marko; Radisek, Sebastjan; Tian, Hui; Hein, Ingo

Published in:
Molecular Plant-Microbe Interactions

DOI:
[10.1094/MPMI-03-19-0079-R](https://doi.org/10.1094/MPMI-03-19-0079-R)

Publication date:
2019

Document Version
Peer reviewed version

[Link to publication in Discovery Research Portal](#)

Citation for published version (APA):
Volk, H., Marton, K., Flajsman, M., Radisek, S., Tian, H., Hein, I., Podlipnik, ., Thomma, B. P. H. J., Kosmelj, K., Javornik, B., & Berne, S. (2019). Chitin-Binding Protein of *Verticillium nonalfalfae* Disguises Fungus from Plant Chitinases and Suppresses Chitin-Triggered Host Immunity. *Molecular Plant-Microbe Interactions*, 32(10), 1378-1390. <https://doi.org/10.1094/MPMI-03-19-0079-R>

General rights

Copyright and moral rights for the publications made accessible in Discovery Research Portal are retained by the authors and/or other copyright owners and it is a condition of accessing publications that users recognise and abide by the legal requirements associated with these rights.

- Users may download and print one copy of any publication from Discovery Research Portal for the purpose of private study or research.
- You may not further distribute the material or use it for any profit-making activity or commercial gain.
- You may freely distribute the URL identifying the publication in the public portal.

Take down policy

If you believe that this document breaches copyright please contact us providing details, and we will remove access to the work immediately and investigate your claim.

1 Chitin binding protein of *Verticillium* 2 *nonalfalfae* disguises fungus from plant 3 chitinases and supresses chitin-triggered 4 host immunity

5 Helena Volk¹, Kristina Marton¹, Marko Flajšman¹, Sebastjan Radišek², Hui Tian³, Ingo Hein^{4,5}, Črtomir
6 Podlipnik⁶, Bart P.H.J. Thomma³, Katarina Košmelj¹, Branka Javornik¹, Sabina Berne¹

7 ¹Department of Agronomy, Biotechnical Faculty, University of Ljubljana, Jamnikarjeva 101, SI-1000
8 Ljubljana, Slovenia; ²Slovenian Institute of Hop Research and Brewing, Cesta Žalskega tabora 2, SI-3310
9 Žalec, Slovenia; ³Laboratory of Phytopathology, Wageningen University and Research,
10 Droevendaalsesteeg 1, 6708 PB Wageningen, the Netherlands, ⁴The James Hutton Institute, Invergowrie,
11 Dundee DD2 5DA, Scotland, United Kingdom; ⁵The University of Dundee, School of Life Sciences, Division
12 of Plant Sciences at the JHI, Invergowrie, Dundee DD2 5DA, Scotland, United Kingdom; ⁵Department of
13 Chemistry and Biochemistry, Faculty of Chemistry and Chemical Technology, University of Ljubljana,
14 Večna pot 113, SI-1000 Ljubljana, Slovenia

15
16 Corresponding author: S. Berne; E-mail: sabina.berne@bf.uni-lj.si

17
18 Nucleotide sequence data is available under accession numbers MH325205 for *VnaChtBP*, and
19 MH325206 for *VaChtBP*.

20 **Abstract**

21 During fungal infections, plant cells secrete chitinases, which digest chitin in the fungal cell walls. The
22 recognition of released chitin oligomers via lysin motif (LysM)-containing immune host receptors results
23 in the activation of defence signalling pathways. We report here that *Verticillium nonalfalfae*, a
24 hemibiotrophic xylem-invading fungus, prevents these digestion and recognition processes by secreting
25 a CBM18 (carbohydrate binding motif 18)-chitin binding protein, VnaChtBP, which is transcriptionally
26 activated specifically during the parasitic life stages. VnaChtBP is encoded by the *Vna8.213* gene, which is
27 highly conserved within the species, suggesting high evolutionary stability and importance for the fungal
28 lifestyle. In a pathogenicity assay, however, *Vna8.213* knockout mutants exhibit wilting symptoms similar
29 to the wild type fungus, suggesting that *Vna8.213* activity is functionally redundant during fungal
30 infection of hop. In a binding assay, recombinant VnaChtBP binds chitin and chitin oligomers *in vitro* with
31 submicromolar affinity and protects fungal hyphae from degradation by plant chitinases. Moreover, the
32 chitin-triggered production of reactive oxygen species from hop suspension cells was abolished in the
33 presence of VnaChtBP, indicating that VnaChtBP also acts as a suppressor of chitin-triggered immunity.

34 Using a yeast-two-hybrid assay, circular dichroism, homology modelling and molecular docking, we
35 demonstrated that VnaChtBP forms dimers in the absence of ligands and that this interaction is
36 stabilized by the binding of chitin hexamers with a similar preference in the two binding sites. Our data
37 suggest that, in addition to chitin binding LysM (CBM50) and Avr4 (CBM14) fungal effectors, structurally
38 unrelated CBM18 effectors have convergently evolved to prevent hydrolysis of the fungal cell wall
39 against plant chitinases and to interfere with chitin-triggered host immunity.

40 **Introductory statements**

41 Plant defense against pathogenic organisms relies on innate immunity, which is triggered by recognition
42 of pathogen-derived or endogenous danger signals by plant receptors, described as pattern-triggered
43 immunity (PTI) and effector-triggered immunity (ETI) (Jones and Dangl 2006; Dodds and Rathjen 2010).
44 PTI is activated by host cell surface-localized pattern recognition receptors (PRRs) sensing pathogen- and
45 danger-associated molecular patterns (PAMPs and DAMPs, respectively) (Boller and Felix 2009; Böhm et
46 al. 2014). Pattern recognition receptors, which are either receptor-like kinases (RLKs) or receptor-like
47 proteins (RLPs) that function in conjunction with RLKs, sense PAMPs or DAMPs and transduce
48 downstream signaling to trigger PTI responses. Early PTI responses include the rapid generation of
49 reactive oxygen species, the activation of ion channels and mitogen-activated protein kinases. In turn,
50 this leads to the expression of defense related genes, leading to an accumulation of antimicrobial
51 compounds such as enzymes, which damage pathogen structures, inhibitors of pathogen enzymes and
52 other antimicrobial molecules (Macho and Zipfel 2014; Boller and Felix 2009; Dodds and Rathjen 2010).

53 PAMPs, released during infection, are conserved molecular patterns characteristic of different pathogen
54 classes (Ranf 2017). In fungi, chitin, in addition to beta-glucan and xylanase, is a well-studied PAMP that
55 activates the host defense response (Sanchez-Vallet et al. 2014). Chitin (a polymer of β -1,4-linked N-
56 acetylglucosamine; (GlcNAc)_n), is a major and highly conserved component of fungal cell walls and can be
57 degraded to chitin oligosaccharides by plant apoplastic chitinases (Punja and Zhang 1993; Pusztahelyi
58 2018). The generated chitin fragments are recognized by a chitin perception system and subsequently
59 activate PTI (Shibuya and Minami 2001; Shinya et al. 2015; Sanchez-Vallet et al. 2014).

60 Major chitin sensing PRRs, RLKs and RLPs belonging to the LysM domain family, are well studied in
61 *Arabidopsis* and rice (Gust et al. 2012; Ranf 2017). *Arabidopsis* LysM-RLK AtCERK1 (chitin elicitor receptor
62 kinase1) binds N-acetylated chitin fragments with three LysM motifs and, through homodimer
63 formation, mediates chitin-inducible plant defenses (Miya et al. 2007; Liu et al. 2012). Cao et al. (2014)
64 later identified another LysM-RLK in *Arabidopsis*, AtLYK5, which binds chitin at a higher affinity than
65 AtCERK1. The authors propose that AtLYK5 functions as the major chitin receptor, which recruits
66 AtCERK1 to form a chitin inducible receptor complex. In rice, two receptors are involved in chitin
67 triggered immunity (Shimizu et al. 2010). LysM-RLP OsCEBiP (chitin elicitor binding protein) binds N-
68 acetylated chitin fragments, which initiates receptor homodimerization and further heterodimerization
69 with OsCERK1. This heterotetramer formation triggers chitin induced PTI (Hayafune et al. 2014).

70 To overcome chitin-triggered immunity, successful pathogens have evolved various strategies, including
71 alteration of the composition and structure of cell walls, modification of carbohydrate chains and

72 secretion of effector proteins to prevent hydrolysis of the fungal cell wall or the release and recognition
73 of chitin oligosaccharides (Sanchez-Vallet et al. 2014).

74 A well-described strategy of fungal cell wall protection against host chitinases is that of the tomato leaf
75 mold fungus *Cladosporium fulvum*, which secretes chitin-binding protein Avr4 during infection. Avr4
76 effector binds with its carbohydrate-binding module family 14 (CBM14) to the fungal cell wall chitin and
77 thus shields fungal hyphae against degradation by chitinases (van den Burg et al. 2007; van Esse et al.
78 2007). There is evidence of a similar protection of cell wall chitin in a phylogenetically closely related
79 species of the Dothideomycete fungi class harboring homologs of Avr4 (Stergiopoulos et al. 2010).
80 Protection of fungal hyphae against hydrolysis by chitinases has also been shown for fungal effectors
81 Mg1LysM and Mg3LysM of *Zymoseptoria tritici* (formerly *M. graminicola*) (Marshall et al. 2011) and
82 Vd2LysM from *Verticillium dahliae* (Kombrink et al. 2017), one of the LysM fungal effectors (de Jonge and
83 Thomma 2009) that are known to bind chitin oligomers via LysM domains or carbohydrate-binding
84 module family 50 (CBM50) (Akcipinar et al. 2015). The first LysM effector, Ecp6, was found in the
85 tomato pathogen *C. fulvum* and its characterization provided evidence that Ecp6 specifically and with
86 high affinity binds chitin oligosaccharides. This competition with receptors subsequently disrupts chitin
87 recognition by host receptors and suppresses the chitin-triggered immune response (Bolton et al. 2008;
88 de Jonge et al. 2010; Sanchez-Vallet et al. 2013). Some fungal genomes contain several genes for LysM
89 effectors and those highly expressed during infection have been characterized in fungal pathogens,
90 including *Z. tritici* (Marshall et al. 2011), *Magnaporthe oryzae* (Mentlak et al. 2012), *Colletotrichum*
91 *higginsianum* (Takahara et al. 2016) and *V. dahliae* (Kombrink et al. 2017). These studies demonstrate
92 the involvement of LysM effectors in shielding fungal hyphae from chitinases, blocking chitin-induced
93 plant defense responses and in pathogen virulence, or in a combination of these effects.

94 The question arises of whether there are other molecules/systems/complexes apart from Avr4 (CBM14)
95 and LysM (CBM50) effectors, which can interfere with plant chitin perception and activation of PTI. We
96 have been studying the *Verticillium nonalfalfae* – hop (*Humulus lupulus* L.) pathosystem. In an early
97 comparative transcriptomic study of compatible and incompatible interactions (Cregeen et al. 2015), an
98 *in planta* expressed *V. nonalfalfae* lectin gene was detected. Its relative expression was increasing in
99 susceptible hop cultivar ‘Celeia’ and decreasing in resistant cultivar ‘Wye Target’ over the time course of
100 infection. A preliminary study showed that this *V. nonalfalfae* lectin contains putative carbohydrate-
101 binding module family 18, CBM18 (Wright et al. 1991) domains. CBM18 is a chitin-binding domain
102 involved in recognition of chitin oligomers and typically found in fungal and plant proteins in one or more
103 copies (Lerner and Raikhel 1992). We report here on the characterization of *V. nonalfalfae* lectin with six
104 CBM18 domains and show that it is a novel effector in plant fungal pathogens. VnaChtBP binds chitin,
105 suppresses chitin-triggered production of reactive oxygen species (ROS) in hop and protects hyphae of
106 *Trichoderma viride* from hop chitinases in an *in vitro* protection assay.

107

108 Results

109 The majority of CBM18 module containing proteins of *V. nonalfalfae* are expressed in 110 *planta*

111 The *Vna8.213* gene, encoding a putative pathogen CBM18-containing chitin binding protein (*VnaChtBP*),
112 has previously been identified as a differentially expressed transcript during compatible and
113 incompatible interactions of *V. nonalfalfae* and hop (Cregeen et al. 2015). Surveying the *V. nonalfalfae*
114 genome, (Jakše et al. 2018) uncovered ten additional genes that encode for proteins with at least one
115 CBM18 module (Fig. 1). These genes were grouped into four categories according to their domain
116 architecture: Lectin-like proteins (Fig. 1 A), Chitinases (Fig. 1 B), Chitin deacetylases (Fig. 1 C) and
117 Xyloglucan endotransglucosylase (Fig. 1 D). The size of these proteins ranged between 349 and 1,696
118 amino acids (*Vna6.1* and *Vna1.668*, respectively) and they harbored between one and ten CBM18
119 modules. Of these genes, ten are differentially expressed *in planta* (Fig. 1 E) (Marton et al. 2018) and five
120 (*Vna2.980*, *Vna6.6*, *Vna8.213*, *Vna9.506* and *Vna9.510*) were predicted to be classically secreted proteins
121 with N-terminal signal peptides. Of the chitinases (Fig. 1 B), transcripts of *Vna3.655* and *Vna9.506* were
122 detected exclusively in susceptible hop, *Vna1.668* transcripts were found expressed in the roots of both
123 resistant ('Wye Target') and susceptible ('Celeia') hop varieties, while transcripts of *Vna2.980* and
124 *Vna9.510* were barely detectable. Interestingly, only one chitin deacetylase gene (*VnaUn.355*) was
125 expressed during infection, and it showed preferential induction in the roots of both hop varieties. Such
126 an expression profile was also evident for transcripts of *Vna6.6* belonging to xyloglucan
127 endotransglucosylase. The highest expression was observed for *Vna8.213* transcripts, in particular at the
128 late stages of infection of susceptible hop. Interestingly, the *Vna1.667* gene-encoding lectin-like protein,
129 containing 10 CBM18 modules, was barely expressed in the roots of susceptible hop during the early
130 infection stages.

131 In addition to chitinases (Fig. 1 B), which contain the family 18 glycoside hydrolase domain, one CBM18
132 and 2-3 CBM50 chitin-binding modules known as LysM domains, another group of protein-like LysM
133 effectors (de Jonge and Thomma 2009) is encoded in the *V. nonalfalfae* genome. Seven genes harboring
134 1-6 LysM domains were found, four of them with signal peptide and five of them showing expression in
135 infected hops (e-Xtra Fig. S1). The highest expression *in planta* was determined for *Vna2.731*, which is
136 predicted to encode a 19.3 kDa protein with the 1 transmembrane domain and 1 LysM domain and
137 shares 99% identity with the VDBG_03944 protein from *V. alfalfae* VaMs.102.

138 To confirm the expression patterns of *Vna8.213* measured by RNA-Seq, detailed gene expression
139 profiling of root and shoot samples from susceptible and resistant hop varieties was performed using RT-
140 qPCR at 6, 12 and 18 days post-inoculation (dpi) with *V. nonalfalfae* (Fig. 2). Gene expression of
141 *Vna8.213*, hereinafter designated *VnaChtBP*, increased with time, reaching the highest abundance in
142 stems of susceptible hop at 18 dpi. The overall *VnaChtBP* expression in resistant hop was at a much
143 lower level than in the susceptible variety and peaked at 12 dpi in stems. These results indicate that
144 *VnaChtBP* expression is induced *in planta* and its transcript abundance in susceptible hop increases with
145 the progression of fungal colonization.

146 Sequence conservation suggests evolutionary stability of *VnaChtBP*

147 To investigate the presence and sequence variation of *VnaChtBP* in 28 *V. nonalfalfae* isolates (e-Xtra
148 Table S1), PCR amplification and Sanger sequencing of cloned genes was performed. The *VnaChtBP* gene
149 was present in all analyzed isolates and displayed no sequence polymorphisms. This suggests the
150 evolutionary stability of the gene, as well as an important role in the fungal lifestyle.

151 Among all sequences deposited at NCBI, *VnaChtBP* shared the highest protein identity with a lectin from
152 *V. alfalfae* (97%; an alfalfa isolate VaMs.102), followed by *V. dahliae* lectin-B (80%; a lettuce isolate
153 VdLs.17), two *V. dahliae* hypothetical proteins, Vd0004_g7043 and Vd0001_g7025 (80% and 79%;
154 strawberry isolates 12161 and 12158), and a hypothetical protein BN1708_012400 from *V. longisporum*
155 (78%; a rapeseed isolate VL1) (e-Xtra Table S2). Additional homologs (e-Xtra File S1), but with lower
156 identity (48-39%), were identified in fungi amongst Sordariomyceta (40) and Dotideomyceta (3), and in
157 fungi *Incertae sedis* amongst Neocallimastigomycetes (5) and Chytridiomycetes (2).

158 Because of the high sequence similarity shared between *VnaChtBP* and *V. alfalfae* VaMs.102 lectin, PCR
159 screening and Sanger sequencing of amplicons from four additional *V. alfalfae* isolates was carried out.
160 As with *VnaChtBP*, no allelic polymorphisms were found among the sequences obtained and comparison
161 of *V. nonalfalfae* and *V. alfalfae* gene sequences from these isolates also showed 97% sequence identity.
162 Within the 36 single nucleotide polymorphisms identified, only 13 resulted in amino acid substitutions
163 (e-Xtra File S2).

164 *VnaChtBP* binds chitin *in vitro* and protects fungal hyphae against plant chitinases

165 *V. nonalfalfae VnaChtBP* is an intronless gene and predicted to encode for a cysteine rich (12.5%)
166 apoplastic effector (*VnaChtBP*) with 400 amino acids, including N-terminal signal peptide and six type 1
167 Chitin binding domains (ChtBD1; PF00187). This domain is classified in the CAZY database (Lombard et al.
168 2014) as Carbohydrate-binding module 18 (CBM18) and consists of 30 to 43 residues rich in glycines and
169 cysteines, which are organized in a conserved four-disulfide core (Andersen et al. 1993; Asensio et al.
170 2000; Wright et al. 1991). It is a common structural motif, with a consensus sequence
171 X3CGX7CX4CCSX2GXCGX5CX3CX3CX2 (Prosite PS50941), found in various plant and fungal defense
172 proteins and is involved in the recognition and/or binding of chitin subunits (Finn et al. 2014).

173 To confirm carbohydrate binding, *E. coli* produced and Ni-NTA affinity purified recombinant *VnaChtBP* (e-
174 Xtra Fig. S2) was used in a sedimentation assay with various carbohydrates. *VnaChtBP* bound specifically
175 to chitin polymer, in the form of chitin beads and crab shell chitin, but not to the plant cell wall polymers
176 cellulose and xylan (Fig. 3). To examine the affinity of *VnaChtBP* binding to chitin in more detail,
177 recombinant protein was immobilized to the CM5 sensor chip and the *VnaChtBP* interaction with chitin
178 hexamer was analyzed using surface plasmon resonance (SPR) (Kastritis and Bonvin 2013). *VnaChtBP*
179 revealed concentration-dependent binding of chitin hexamer (Fig. 4) with a dissociation constant of 0.78
180 ± 0.58 μM , while no specific binding to other tested carbohydrates was detected (e-Xtra Fig. S3). Since
181 the chitin binding affinity of the protein increases for longer chitin oligomers (Asensio et al. 2000), this
182 value is comparable to other reported chitin oligomer binding affinities of fungal effectors but exceeds
183 by one order of magnitude those reported for *Arabidopsis* chitin recognition receptors and hevein (Table
184 1). reported to protect fungal hyphae from plant chitinases (Van Den Burg et al. 2004; Marshall et al.

2011). To determine whether recombinant VnaChtBP can protect fungal cell walls against hydrolysis by plant chitinases, a cell protection assay adapted from Mentlak et al. (2012) was performed using germinating conidia of *Trichoderma viride*. Xylem sap extracted from *V. nonalfalfae* infected hop (Flajšman et al. 2018) was used as a source of plant chitinases. Chitinase activity was determined as a release of soluble Remazol brilliant violet 5R dye hydrolyzed from insoluble Chitin Azure substrate. The extracted xylem sap contained 19 U of active chitinase per mg of total protein. In the presence of xylem sap, only minimal germination of the *T. viride* conidia occurred after 24 h incubation, while pre-incubation in a 3 μ M solution of recombinant VnaChtBP prior to the addition of xylem sap enabled germination of conidia and hyphal growth. Interestingly, aggregation and compaction of fungal hyphae were detected only in the presence of both xylem sap and VnaChtBP, while normal mycelial growth without hyphal aggregation was observed in the solution of VnaChtBP (Fig. 5). We assume that VnaChtBP, by binding and probably surrounding chitin fibers in the fungal cell wall, masks chitin and protects it from degradation by xylem sap chitinases.

198 VnaChtBP suppresses chitin-triggered plant immunity in hop

199 Several fungal chitin binding effectors prevent chitin mediated PTI trigger (Mentlak et al. 2012; Sanchez-
200 Vallet et al. 2013; Takahara et al. 2016). To test whether VnaChtBP interferes with plant immune
201 responses by sequestering chitin oligomers in the apoplast, the reactive oxygen species (ROS) released
202 from the hop suspension cells in response to (GlcNAc)₆, in the presence or absence of VnaChtBP, were
203 measured using a chemiluminescent assay. Treatment of hop suspension cells with 1 μ M (GlcNAc)₆
204 resulted in a strong production of ROS, whereas this response was completely abolished in the presence
205 of 5 μ M VnaChtBP (Fig. 6).

206 It appears that similar to LysM effectors, CBM18-containing effector VnaChtBP can suppress chitin-
207 triggered generation of ROS and perturb plant immune responses.

208 VnaChtBP forms dimers and has two potential binding sites for interaction with 209 chitin

210 Since many chitin binding proteins have been reported to form dimers (Liu et al. 2012; Sanchez-Vallet et
211 al. 2013; Cao et al. 2014), a yeast-two-hybrid assay was carried out using *VnaChtBP* as both bait and prey
212 to study the ability to dimerize. Dimer formation of VnaChtBP was detected on a minimal medium using
213 histidine as a reporter (Fig. 7 A). Consistent with a weak interaction, only limited growth was observed
214 on triple dropout reporter medium (synthetic complete medium without leucine, tryptophan and uracil)
215 and the X-gal reporter was not activated. Far UV CD spectra of VnaChtBP in the presence and absence of
216 chitin hexamer were obtained to show that binding of chitin to VnaChtBP induces additional secondary
217 structure formation (Fig. 7 B). Based on the shape of the spectrum, the secondary structure is
218 predominantly alpha helical.

219 To understand the chitin binding mechanism of CBM18 effectors better, homology modelling of the
220 VnaChtBP 3D structure was performed. The SWISS-MODEL server produced three models based on
221 different templates, shown in Table 2. Model02 provided the best fit for four out of six CBM18 modules
222 and was used as the basis of the characterization. Molecular docking of the chitin hexamer into the
223 VnaChtBP model (Fig. 7 C) shows that each protein monomer contributes to the formation of two

224 binding sites accessible to the ligand. In binding site I (BSI), chitin hexamer is accommodated in a shallow
225 groove formed by four hevein domains of polypeptide chain A and two hevein domains of chain B, while
226 binding site II (BSII) is comprised of four hevein domains of chain B and two domains of chain A.
227 According to the analysis of the presented complex with YASARA, the binding of chitin hexamer in BSI is
228 strengthened by eleven (four accepted and seven donated) hydrogen bonds and eight hydrophobic
229 interactions, which contribute to the total binding energy of 6.891 kcal/mol (AutoDock/Vina) and an
230 estimated docking score of 8.88 μ M. A similar preference for binding of chitin hexamer in the BSII was
231 observed, with an estimated docking score of 2.01 μ M and a total binding energy of 7.772 kcal/mol,
232 supported by eight (three accepted, five donated) hydrogen bonds and 12 hydrophobic interactions
233 between the ligand and receptor.

234 *VnaChtBP* deletion has no significant effect on the growth and pathogenicity of *V.* 235 *nonalfalfae*

236 Since *VnaChtBP* is specifically expressed during colonization of hop, its contribution to fungal virulence
237 was tested in the susceptible hop variety 'Celeia'. *V. nonalfalfae* knockout mutants of *VnaChtBP* were
238 generated by targeted gene disruption via *A. tumefaciens*-mediated transformation. Prior to plant
239 inoculation, growth of fungal colonies and sporulation of knockout mutants were assessed *in vitro* and
240 compared to the wild type (e-Xtra Fig. S4 A). In the selected knockout mutants, mycelial growth and
241 fungal morphology did not differ significantly from the wild type. Reduced sporulation was observed for
242 both mutants compared to the wild type but this did not impact on disease frequency. After inoculation
243 of the hop plants, disease symptoms were independently assessed five times using a disease severity
244 index (DSI) with a 0-5 scale (Radišek et al. 2003). After the final symptom assessment, the presence of
245 fungus in all inoculated plants was confirmed through re-isolation tests. In addition, no differences in the
246 relative amount of fungal DNA between the wild type and *VnaChtBP* mutant strains (e-Xtra Fig. S4 B)
247 were observed on the basis of fungal biomass quantification in infected hop at 21 dpi.

248 Disease symptoms were monitored in susceptible hop following infection with the wild type *V.*
249 *nonalfalfae* and knockout mutants of *VnaChtBP* (Fig. 8 A). Both *VnaChtBP* mutants displayed *Verticillium*
250 wilting symptoms (chlorosis and necrosis of the leaves) in susceptible hop similar to the wild type fungus,
251 with no significant differences among them according to the disease severity index (DSI) assessment (Fig.
252 8 B). Independent pathogenicity assays with additional *VnaChtBP* deletion mutants yielded the same
253 results (data not shown). This suggests that the *VnaChtBP* function is redundant for *V. nonalfalfae*
254 infection.

255 Discussion

256 *V. nonalfalfae*, a soil born fungal pathogen, causes serious economic damage in European hop growing
257 regions. Significant efforts have been invested in studying the molecular mechanisms of *Verticillium* wilt
258 in hop and fungus pathogenicity (Radišek et al. 2006; Jakše et al. 2013; Mandelc and Javornik 2015;
259 Flajšman et al. 2016; Cregeen et al. 2015; Jakše et al. 2018; Marton et al. 2018).

260 *In planta* expressed fungal proteins are potential effector candidates that might be implicated in
261 pathogen virulence. The effector candidate *V. nonalfalfae VnaChtBP* studied here, encodes for a CBM18

262 domain containing chitin binding protein and is highly expressed in hop plants. Using an established
263 bioinformatic pipeline (Marton et al. 2018), we identified eleven genes in the *V. nonalfalfae* genome that
264 contain CBM18 domains. Of these genes, two harboured a single CBM18 domain and five, including
265 *VnaChtBP*, contain a predicted N-terminal signal peptide. Although CBMs play a key role in the
266 recognition of carbohydrates and are known to promote efficient substrate hydrolysis as a part of
267 carbohydrate-active enzymes (e.g., CBM18 motifs found in chitinases), they have also been found to be
268 present in toxins, virulence factors and pathogenesis-associated proteins (Guillén et al. 2010). Proteins
269 containing CBM18 motifs are common in fungi, particularly in plant and animal pathogens. Indeed, they
270 are almost three times as common in the proteomes of pathogens than in those of non-pathogenic fungi
271 across the phylum Ascomycota (Soanes et al. 2008). Intriguingly, in *Verticillium* spp., CBM18 containing
272 genes are more frequently observed in mild pathogenic *V. tricorpus* (13) (Seidl et al. 2015) than in high
273 pathogenic *V. dahliae* and *V. alfalfae* (9). The expansion of CBM18 domains in ChtBPs may be linked to
274 the evolution of pathogenicity, and has, for example, been reported in the fungal pathogen *B.*
275 *dendrobatidis*, which has caused a worldwide decline of amphibian populations (Abramyan and Stajich
276 2012). In total, eighteen genes with between one to eleven CBM18 domains have been identified in *B.*
277 *dendrobatidis*, including some classified as lectin-like proteins. Biochemical characterization of three
278 such lectin-like proteins revealed that two have a signal peptide and co-localize with chitinous cell wall in
279 *Saccharomyces cerevisiae*. Furthermore, one of these proteins has been shown to bind chitin and
280 thereby protect *Trichoderma reesei* from exogenous chitinase, suggesting a role of lectin-like proteins in
281 fungal defence (Liu and Stajich 2015). Similarly, in the rice blast fungus *M. oryzae*, 15 genes with one to
282 four CBM18 domains were found, although gene-targeted disruption and tolerance to chitinase
283 treatment did not support the implication of the tested genes in fungal pathogenicity (Mochizuki et al.
284 2011).

285 *VnaChtBP* consists of six tandemly repeated CBM18 motifs, contains a signal peptide and is predicted to
286 reside in the apoplast, which is consistent with the role of chitin binding in the extracellular space.
287 Homology search of proteins that contain CBM18 motifs in other *Verticillium* species revealed that this
288 type of protein is common in pathogenic *Verticillium* species but it seems not to be ubiquitous. For
289 example, in the recently sequenced genomes of five *V. dahliae* strains isolated from strawberry, three
290 strains harbored ChtBPs with five, six and ten CBM18 motifs, while none were detected in the two other
291 strains.

292 Monitoring the *in planta* expression of *VnaChtBP* showed that it is highly expressed at the later stages of
293 infection in a susceptible hop cultivar, and continues to be expressed even at 30 dpi, when plants exhibit
294 severe wilting symptoms (Cregeen et al. 2015; Marton et al. 2018). In contrast, in a resistant cultivar, the
295 *VnaChtBP* gene is slightly induced after infection and then completely down-regulated. The expression
296 pattern of the *VnaChtBP* gene coincides with *V. nonalfalfae* colonization of hop, whereby the fungus
297 spread is unimpeded in susceptible plants, while colonization is arrested around 12-20 dpi in resistant
298 hop plants, presumably due to strong plant resistance responses (Cregeen et al. 2015). The immune
299 reaction in the incompatible interaction is unlikely to impose selection pressure on the *VnaChtBP* gene
300 since no allelic polymorphisms were detected among the analysed *V. nonalfalfae* isolates. Similarly, no
301 allelic variation was found in the closest (97% identity) homolog to the *VnaChtBP* gene from isolates of *V.*

302 *alfalfae*, suggesting highly conserved genes. Allelic variation is commonly detected in fungal proteins that
303 function as avirulent (Avr) determinants on perception by the host defence, but not necessarily in
304 virulence factors of the pathogen (Stergiopoulos et al. 2007). Taken together, we speculate that the
305 absence of allelic variation and the high gene expression observed *in planta* suggest a role for VnaChtBP
306 in the virulence of *V. nonalfalfae*. However, in a pathogenicity assay, *VnaChtBP* targeted deletion
307 mutants were not significantly impaired in their hops infectivity compared to wild type fungus which is in
308 line with functional redundancy. Unchanged virulence of deletion mutants, presumably due to functional
309 redundancy, has been reported for two other tested CBM18-containing ChtBPs in *M. oryzae* (Mochizuki
310 et al. 2011) and also for LysM fungal effector, Mg1LysM, of *Mycosphaerella graminicola* (Marshall et al.
311 2011). Indeed, seven putative chitin binding LysM effectors have been found in the *V. nonalfalfae*
312 genome, which may have a role in protection of the fungal cell wall chitin or may interfere with chitin-
313 triggered plant immunity. Orthologues of *C. fulvum* Avr4 with the CBM14 chitin-binding motif were not
314 identified in the *V. nonalfalfae* genome (Jakše et al. 2018) or in the predicted proteomes of other
315 *Verticillium* species (Seidl et al. 2015).

316 Consistent with previously characterized CBM18 containing proteins from *M. oryzae* (Mochizuki et al.
317 2011) and *B. dendrobatidis* (Liu and Stajich 2015), recombinant VnaChtBP binds specifically to chitin
318 beads and crab shell chitin, but not to plant cell wall cellulose or xylan. In addition to chitin polymer,
319 recombinant VnaChtBP also bound chitin hexamer in an SPR experiment, with binding affinity in the
320 submicromolar range. Compared to plant chitin receptors, recombinant VnaChtBP together with LysM
321 effectors Ecp6 from *C. fulvum*, Slp1 from *M. oryzae* (Mentlak et al. 2012) and ChELP1 and ChELP2 from *C.*
322 *higginsianum* (Takahara et al. 2016), exhibit three to five orders of magnitude higher affinity to chitin
323 oligomers. It is thus not surprising that these fungal effectors are able to outcompete plant chitin
324 receptors, such as *Arabidopsis thaliana* AtLYK5 (Cao et al. 2014) and AtCERK1 (Liu et al. 2012).

325 Based on NMR studies and solved crystal structures of plant LysM chitin receptors, several mechanisms
326 for binding of chitin have been proposed; from a simple 'continuous groove' model for AtCERK1 (Liu et
327 al. 2012) to the OsCEBiP 'sandwich' (Hayafune et al. 2014) and 'sliding mode' model (Liu et al. 2016).
328 However, these models have been unable to explain the observed elicitor activities of chitin oligomers.
329 Building on these models and using a range of chitosan polymers and oligomers bound to *Atcerk1*
330 mutants resulted in an improved 'slipped sandwich' model that fits all experimental results (Gubaeva et
331 al. 2018). A recent structural study of fungal LysM effector Ecp6 from *C. fulvum* revealed a novel chitin
332 binding mechanism that explained how LysM effectors can outcompete plant host receptors for chitin
333 binding (Sanchez-Vallet et al. 2013). Ecp6 consists of three tightly packed LysM domains, with a
334 typical $\beta\alpha\alpha\beta$ fold. Intra-chain dimerization of chitin-binding regions of LysM1 and LysM3 leads to the
335 formation of a deeply buried chitin binding groove with an ultra-high (pM) affinity. The remaining LysM2
336 domain also binds chitin, albeit with low micromolar affinity, and interferes with chitin-triggered
337 immunity, possibly by preventing chitin immune receptor dimerization and not by chitin fragment
338 sequestering, as in the case of LysM1-LysM3.

339 To date, to the best of our knowledge, the molecular mechanism of chitin binding of CBM18 fungal
340 effectors remains elusive. However, the 3D homology model of VnaChtBP provides a tangible model for
341 the molecular docking of the chitin hexamer. Although only four out of six CBM18 domains could be

342 reliably modelled, the analysis revealed that VnaChtBP dimerizes. Importantly, this prediction was
343 independently validated through a yeast-two-hybrid experiment. The VnaChtBP complex has two
344 putative chitin binding sites, which form a shallow binding cleft by cooperation of the two polypeptide
345 chains and have a similar preference to chitin. As in CBM18 lectin-like plant defence proteins (Jiménez-
346 Barbero et al. 2006), typically represented by a small antifungal protein hevein from the rubber tree
347 (*Hevea brasiliensis*), a network of hydrogen bonds and several hydrophobic interactions occur between
348 VnaChtBP residues and N-acetyl moieties of the chitin oligomer. These are thought to stabilize the
349 interaction and contribute to submicromolar chitin binding affinity, as determined by CD and SPR
350 experiments, respectively. Similarly, the recently solved crystal structure of fungal effector CfAvr4, a
351 CBM14 lectin, in complex with chitin hexamer (Hurlburt et al. 2018), revealed that two effector
352 molecules form a sandwich structure, which encloses two parallel stacked chitin hexamer molecules,
353 shifted by one sugar ring, in an extended chitin binding site. In this complex, the interaction is mediated
354 through aromatic residues and numerous hydrogen bonds, with both side chains and main chains.
355 Interestingly, no intermolecular protein-protein interactions have been observed across the dimer,
356 suggesting ligand induced effector dimerization.

357 Fungal plant pathogens have evolved several strategies to escape the surveillance of chitin-related
358 immune systems (Sanchez-Vallet et al. 2014). The various mechanisms used include conversion of chitin
359 to chitosan by chitin deacetylases and inclusion of α -1,3-glucan in the cell walls, as well as secretion of
360 diverse effectors that can shield the fungal hyphae from hydrolysis by plant chitinases, directly inhibiting
361 their activity, acting as scavengers of chitin fragments or preventing chitin-induced plant immunity.
362 Suppression of chitin-triggered immunity has been demonstrated for some LysM effectors with
363 subnanomolar affinity for chitin oligomers (Mentlak et al. 2012; Sanchez-Vallet et al. 2013; Takahara et
364 al. 2016; Kombrink et al. 2017). Here, we find that VnaChtBP binds to chitin oligomers with
365 submicromolar affinity, preventing free chitin oligomers from binding to plant immune receptors and
366 thus suppressing ROS-related defense responses in hop. A protective role against host chitinases has
367 been shown for secreted effector Avr4 from *C. fulvum*, which binds to fungal cell wall chitin to reduce its
368 accessibility to host chitinases (van den Burg et al. 2007). Similar to CfAvr4, wheat pathogen *M.*
369 *graminicola* secreted effectors Mg1LysM, Mg3LysM and *V. dahliae* effector Vd2LysM protect fungal
370 hyphae from hydrolysis by plant chitinases (Marshall et al. 2011; Kombrink et al. 2017). We provide
371 evidence that, in addition to Avr4 (CBM14) and LysM (CBM50) effectors, structurally unrelated CBM18
372 lectin-like proteins that are found in fungal pathogens of plants (this study) and amphibian pathogens
373 (Liu and Stajich 2015) have evolved a chitin shielding ability against plant chitinases.

374 **Materials and Methods**

375 **Cultivation of microorganisms**

376 *Escherichia coli* MAX Efficiency DH5 α or MAX Efficiency DH10B (both from Invitrogen, ThermoFisher
377 Scientific) were used for plasmid propagation and were grown at 37°C on LB agar plates or liquid
378 medium supplemented with appropriate antibiotics (carbenicillin 100 mg/liter, kanamycin 50 mg/liter or
379 gentamicin 25 mg/liter). *E. coli* Shuffle T7 (New England Biolabs) were propagated at 30°C and protein

380 expression was performed at 16°C. *Trichoderma viride* was obtained from The Microbial Culture
381 Collection Ex (IC Mycosmo (MRIC UL)) and all *Verticillium* strains were from the Slovenian Institute of
382 Hop Research and Brewing fungal collection. Fungi were grown at 24°C in the dark on ½ Czapek-Dox agar
383 plates or liquid medium. Knockout mutants were retrieved from selection medium supplemented with
384 150 mg/liter timentin and 75 mg/liter hygromycin.

385 RNA sequencing

386 RNA-Seq library preparation from *V. nonalfalfae* infected hop at 6, 12, 18 and 30 days post inoculation
387 (dpi) and data processing have been previously described (Progar et al. 2017). Fungal transcripts were
388 filtered out and their gene expression profiles were generated using the Hierarchical clustering with
389 Euclidean distance method in R language (R Core Team 2016). Data were presented as a matrix of
390 log₂CPM (counts per million–number of reads mapped to a gene model per million reads mapped to the
391 library) expression values.

392 *VnaChtBP* gene expression profiling with RT-qPCR

393 The expression of *VnaChtBP* was quantified by RT-qPCR in hop infected with *V. nonalfalfae* isolate T2.
394 Total RNA was extracted at 6, 12, and 18 dpi using a Spectrum Plant total RNA kit (Sigma-Aldrich) and 1
395 µg was reverse transcribed to cDNA using a High Capacity cDNA reverse transcription kit (Applied
396 Biosystems). The qPCR reaction was run in 5 biological and 2 technical replicates on an ABI PRISM 7500
397 (Applied Biosystems), under the following conditions: denaturation at 95°C for 10 min, followed by 40
398 cycles at 95°C for 10 s, 60°C for 30 s, and consisted of: 50 ng of cDNA, 300 nM forward and reverse
399 primer, and 5 µl of Fast SYBR Green master mix (Roche). The results were analyzed using the $\Delta\Delta C_t$
400 method (Schmittgen and Livak 2008). Transcription levels of *VnaChtBP* were quantified relative to its
401 expression in liquid Czapek-Dox medium and normalized to fungal biomass in hop using topoisomerase
402 and splicing factor as reference genes (Marton et al. 2018). One way ANOVA with Tukey's post hoc test
403 was performed to test for differences between the group means. Primers used are listed in e-Xtra Table
404 S3.

405 Genetic analysis

406 Genomic DNA was extracted from 7-10 day PDA cultured *Verticillium* isolates by the CTAB extraction
407 method (Möller et al. 1992). PCR reactions were performed in 50 µl using Q5® High-Fidelity DNA
408 Polymerase (NEB), 500 nM gene-specific primers (e-Xtra Table S3) and 100 ng DNA under the following
409 conditions: denaturation at 95°C for 10 min, followed by 40 cycles at 95°C for 10 s, 58°C for 30 s, 72°C for
410 90 s, and a final elongation step at 72°C for 90 s. PCR products were purified from agarose gel (Silica
411 Bead DNA Gel Extraction Kit, Fermentas), cloned into pGEM®-T Easy vector (Promega) and sequenced
412 using Sanger technology with gene-specific and plasmid-specific primers (e-Xtra Table S3). Sequences
413 were analyzed using CodonCode Aligner V7.1.2 (CodonCode Co.) and deposited at the NCBI.

414 Bioinformatic analysis

415 A putative localization of *VnaChtBP* to the apoplast was predicted with ApoplastP 1.0 (Sperschneider et
416 al. 2018). To classify *V. nonalfalfae* CBM18-containing proteins functionally, sequence based searches
417 were carried out using the FunFHMmer web server at the CATH-Gene3D database (Dawson et al. 2017).

418 To obtain VnaChtBP homologs, the amino acid sequence of VnaChtBP was used as a query for NCBI
419 BLAST+ against UniProt Knowledgebase at Interpro (Li et al. 2015).

420 Yeast-two-hybrid assay

421 Dimerization of VnaChtBP was examined with a yeast-two-hybrid experiment using the ProQuest Y2H
422 system (Invitrogen). To generate bait and prey vectors, the *VnaChtBP* gene was cloned into pDEST22 and
423 pDEST32, respectively, and co-transformed in yeast. The interactors were confirmed by plating the yeast
424 co-transformants on triple dropout reporter medium SC-LWH (synthetic complete medium without
425 leucine, tryptophan and histidine), on triple dropout reporter medium SC-LWU (synthetic complete
426 medium without leucine, tryptophan and uracil) and by performing an X-gal assay. The self-activation
427 test of a pDEST22 construct containing the *VnaChtBP* gene with empty pDEST32 vectors was also
428 performed.

429 3D modelling and molecular docking

430 The SWISS-MODEL (Arnold et al. 2006; Waterhouse et al. 2018) server produced three models based on
431 different templates and Model02 was selected for further modelling. The output protein structure was
432 additionally minimized in explicit water using an AMBER14 force field (Duan et al. 2003) and
433 'em_runclean.mcr' script within YASARA Structure (Krieger and Vriend 2014, 2015). A 3D structure
434 model of chitin hexamer was built with SWEET PROGRAM v.2 (Bohne et al. 1998, 1999), saved as a PDB
435 file and used as a ligand in subsequent molecular docking experiments with AUTODOCK/VINA (Trott and
436 Olson 2010), which is incorporated into YASARA Structure. To ensure the integrity of docking results, 200
437 independent dockings of the ligand to the receptor were performed. The pose with the best docking
438 score was selected for further refinement using 'md_refine.mcr' script provided by YASARA Structure.
439 The final model of the hexameric chitin bound to the VnaChtBP dimer was then used for the analysis.

440 Recombinant protein production

441 *VnaChtBP* DNA without predicted signal peptide (SignalP 4.1) was cloned into a pET32a expression vector
442 using a Gibson Assembly® Cloning Kit (NEB). The protein expression in *E. coli* SHuffle® T7 cells (NEB) was
443 induced at OD₆₀₀ = 0.6 with 1 mM IPTG and incubated overnight at 16°C. The recombinant protein was
444 solubilized from inclusion bodies using a mild solubilization method (Qi et al. 2015). Briefly, pelleted cells
445 were resuspended in cold PBS buffer and disrupted by sonication. After centrifugation, the pellet was
446 washed with PBS, resuspended in urea, frozen at -20°C and allowed to slowly thaw at RT. The
447 recombinant protein was purified using Ni-NTA Spin Columns (Qiagen) according to the manufacturer's
448 protocol, aliquoted and stored in 20 mM Tris (pH 8.0) at -80°C.

449 Carbohydrate sedimentation assay and Western blot detection

450 The carbohydrate sedimentation assay was adapted from (van den Burg et al. 2007). Briefly, 15 µg of
451 recombinant VnaChtBP in 20 mM Tris (pH 8.0) was mixed with 1.5 mg of chitin magnetic beads (NEB),
452 crab shell chitin (Sigma-Aldrich), cellulose (Sigma-Aldrich) or xylan (Apollo Scientific) and incubated at RT
453 for 2 h on an orbital shaker at 350 rpm. The same amount of protein in Tris buffer without added
454 carbohydrates was used as a negative control. After centrifugation (5 min, 13,000 g), the supernatant
455 was collected and the pellet was washed three times with 800 µl 20 mM Tris (pH 8.0) prior to
456 resuspension in 4X Bolt™ LDS Sample Buffer with the addition of reducing agent (Invitrogen).

457 The presence of VnaChtBP in different fractions was determined by WB analysis. Samples (25 μ L) were
458 loaded on a precast Bolt™ 4-12% Bis-Tris gel (Invitrogen) and SDS-PAGE in 1x MOPS running buffer was
459 performed using a Mini Gel Tank (ThermoFisher Scientific) for 30 min at 200 V. Proteins were transferred
460 for 1 h at 30 V to an Invitrolon PVDF membrane (Invitrogen) and Ponceau S stained. The membrane was
461 blocked with 5% BSA in 1x PBS before the addition of the primary antibody His-probe (H-3) (SCBT)
462 (1:1,000). The membrane was incubated overnight at 4°C, washed with 1x PBS and incubated in a
463 solution of secondary Chicken anti-mouse IgG-HRP (SCBT) (1:5,000) for 1 h. Protein bands were detected
464 using Super Signal West Pico (ThermoFisher Scientific) ECL substrate in a GelDoc-It2 Imager (UVP).

465 Surface plasmon resonance

466 The binding of hexa-N-acetyl chitohexaose ((GlcNAc)₆; IsoSep) to VnaChtBP was measured using a
467 Biacore T100 analytical system and CM5 sensor chip (Biacore, GE Healthcare). The CM5 sensor chip was
468 activated using an Amine coupling Kit (GE Healthcare) according to the manufacturer's instructions.
469 VnaChtBP was diluted into 10 mM sodium acetate pH 5.1 to a final concentration of 0.1 mg/ml and
470 injected for five minutes over the second flow cell. The first flow cell was empty and served as a
471 reference cell to control the level of non-specific binding. The final immobilization level was
472 approximately 10,000 response units (RU). The (GlcNAc)₆ stock solution was diluted into a series of
473 concentrations (0.05, 0.1, 0.2, 0.4, 0.8, 1.6, 3.2 and 6.4 μ M) with HBS buffer (10 mM HEPES, 140 mM
474 NaCl, pH 7.4) and assayed to detect direct binding to VnaChtBP. Titration was performed in triplicate. In
475 addition to chitin hexamer, N-acetyl glucosamine, glucosamine, glucose, galactose and mannose were
476 tested at a 500 μ M concentration in HBS buffer. Biacore T100 Evaluation software was used to assess the
477 results. First, the sensorgrams were reference and blank subtracted, then a Steady State Affinity model
478 was applied to calculate the affinity constant (K_d). The average of three repeated experiments was used
479 for final K_d determination.

480 Circular dichroism

481 Far UV CD spectra were recorded on a Jasco J-1500 CD spectrometer from 190 to 260 nm at 25 °C using a
482 0.1 cm path length quartz cuvette. The VnaChtBP concentration in 20 mM Tris (pH 8.0) was 2.5 μ M and
483 hexa-N-acetyl chitohexaose ((GlcNAc)₆, Santa Cruz Biotechnology) was at 25 μ M final concentration.
484 Measurements were performed at a 1 nm interval and 5 nm/min scanning speed by using a 1 nm
485 bandwidth. Final spectra were baseline-corrected and transformed to mean residue ellipticity using a
486 mean residue weight of VnaChtBP of 99.851 Da.

487 Xylem sap extraction and chitinase activity assay

488 Xylem sap was extracted from infected hop plants in a pressure chamber at 0.2 MPa for 120 min
489 (Flajšman et al. 2018). The chitinase activity of xylem sap was determined by mixing 150 μ l of xylem sap,
490 or 100 mM Na-acetate (pH 5.0) buffer as negative control, with 1.5 mg of Chitin Azure (Sigma-Aldrich)
491 dissolved in 150 μ l 100 mM Na-acetate (pH 5.0). The samples were incubated for 150 min at 25°C on a
492 rotary shaker at 70 rpm. An aliquot of 80 μ l was taken immediately (blank sample) and after 150 min.
493 The reaction was stopped with the addition of 20%v/v HCl and samples were centrifuged for 10 min at
494 10,000 g. The chitinase activity of xylem sap in the supernatant was determined by measuring the
495 absorbance of released Remazol Brilliant Blue dye at 575 nm against 100 mM Na-acetate (pH 5.0). One

496 enzyme unit was defined as the amount of chitinase that produced a 0.01 increase in absorbance at 575
497 nm, measured at 25°C and pH 5.0. The total protein concentration of the xylem sap was measured in a
498 10x diluted sample using a Pierce™ BCA Protein Assay Kit (Thermo Scientific) following the standard
499 protocol.

500 Cell Protection Assay

501 The cell protection assay was adapted from Mentlak et al., 2012. *Trichoderma viride* conidia were
502 harvested, diluted to 2,000 conidia/ml in 50 µl ½ Czapek-dox medium and incubated overnight. After
503 germination of the conidia, 25 µl of recombinant VnaChtBP (3 µM final concentration) or an equal
504 volume of storage buffer (20 mM Tris; pH 8.0) were added and the conidial suspensions were incubated
505 for 2 h. Fungal cell wall hydrolysis was triggered by the addition of 25 µl of xylem sap as a source of plant
506 chitinases, while 25 µl of Na-acetate (100 mM; pH 5.0) was used in the control experiment. After 24 h
507 incubation, mycelia formation and fungal growth were examined using a Nikon Eclipse 600 microscope.

508 Reactive oxygen species production

509 Hop suspension cells were prepared from hop tissue culture (obtained from the Slovenian Institute of
510 Hop Research and Brewing) as described previously (Langezaal and Scheffer 1992). Briefly, the internodal
511 segments were cultured on solid MS media supplemented with 1 mg/l 2,4-D and 1 mg/l kinetin and
512 calluses were subcultured every two weeks. For initiation of suspension cell culture, 5 g of fresh callus
513 were resuspended in 50 ml of liquid MS media, grown in the dark at 140 rpm and then maintained by
514 subculturing every two weeks.

515 One week old hop suspension cells were harvested by centrifugation and MS medium was replaced by
516 sterile distilled water prior to ROS measurements. For each treatment, a 150 µl aliquot of suspension
517 cells was mixed with a 150 µl assay solution, containing 100 µM L-012 substrate (Sigma, USA), 40 µg/ml
518 horseradish peroxidase (Sigma, USA) and either 1 µM chitin ((GlcNAc)₆, Santa Cruz Biotechnology), 5 µM
519 VnaChtBP, a combination of 1 µM chitin ((GlcNAc)₆ and 5 µM VnaChtBP, or sterile distilled water as
520 negative control. Luminol-based chemiluminescence measurements were recorded for 30 min at a
521 minimal interval (of 2 min 5 s) in a Synergy H1 microplate reader (BioTek Instruments). Data were
522 baseline-corrected and presented as a median with 95% confidence interval of 5 measurements. R
523 package DescTools (Signorell 2017) was used to calculate the area under the curve. A non-parametric
524 Kruskal-Wallis test with Holm's post hoc analysis was used to test the differences between the chitin-
525 treated group, VnaChtBP-treated group and the chitin plus VnaChtBP group.

526 Pathogenicity assay

527 *VnaChtBP* knockout mutants were generated using the *Agrobacterium tumefaciens* mediated
528 transformation protocol described previously (Flajšman et al. 2016) and primers listed in e-Xtra Table S3.
529 Before the pathogenicity tests were carried out, fungal growth and sporulation were inspected as
530 described previously (Flajšman et al. 2017). Briefly, sporulation of fungal samples from liquid Czapek-Dox
531 medium was assessed using a Thoma cell counting chamber under a light microscope. Wild type strain T2
532 was attributed grade 5 – indicating 100% sporulation (typically reaching 10⁷ spores per ml after 1 week).
533 Sporulation of mutant strains was then compared to that of the wild type on a scale from 0-5, with a 20%
534 interval.

535 For the pathogenicity assay, ten plants of the Verticillium wilt susceptible hop cultivar 'Celeia' were
 536 inoculated by 10-min root dipping in a conidia suspension (5×10^6 conidia/ml) of two arbitrarily selected
 537 *VnaChtBP* knockout mutants. Conidia of the wild type *V. nonalfalfae* isolate T2 served as a positive
 538 control and sterile distilled water was used as a mock control. Re-potted plants were grown under
 539 controlled conditions in a growth chamber (Flajšman et al. 2017). Verticillium wilting symptoms were
 540 assessed five times over seven weeks post-inoculation using a disease severity index (DSI) with a 0-5
 541 scale (Radišek et al. 2003). After symptom assessment, a fungal re-isolation test (Flajšman et al. 2017)
 542 was performed to confirm infection of the tested hop plants.

543 In addition, fungal biomass quantification was carried out in five hop plants infected with either wild
 544 type or *VnaChtBP* mutant *V. nonalfalfae* strains. Samples were collected at 21 dpi and total genomic DNA
 545 was extracted using the CTAB protocol (Möller et al. 1992). Fungal DNA was quantified on the Applied
 546 Biosystems® 7500 real-time quantitative PCR system (Applied Biosystems) using Fast SYBR® Green
 547 technology (Thermo Fisher Scientific) and *V. nonalfalfae* lethal genotype (PG2) specific primer 5-1gs
 548 (Radišek et al. 2004). The relative quantity of *V. nonalfalfae* DNA in infected hop was estimated with the
 549 $2^{-\Delta\Delta Ct}$ method (Schmittgen and Livak 2008) using the hop reference gene DRH1 (DEAD box RNA helicase)
 550 for normalization (Štajner et al. 2013). One-way ANOVA with Tukey's multiple comparison test was
 551 performed in GraphPad Prism 8.02 (GraphPad Software, San Diego, California USA, www.graphpad.com)
 552 to test for differences between the wild type and mutant group means.

553 Acknowledgments

554 This research was supported by the Slovenian Research Agency grants P4-0077, J4-8220 and fellowship
 555 342257. This work benefitted from interactions promoted by the COST Action FA 1208 [https://cost-](https://cost-sustain.org)
 556 [sustain.org](https://cost-sustain.org). The authors would like to thank Dr Vasja Progar for transcriptome analysis, Dr Vesna Hodnik
 557 for SPR analysis and Dr Miles Armstrong, Miha Bahun, Urban Kunej, Dr Marko Dolinar, Dr Jernej Jakše
 558 and Dr Nataša Poklar Ulrih for technical advice.

559 Literature Cited

- 560 Abramyan, J., and Stajich, J. E. 2012. Species-specific chitin-binding module 18 expansion in the
 561 amphibian pathogen *Batrachochytrium dendrobatidis*. *MBio*. 3:e00150-12
- 562 Akcapinar, G. B., Kappel, L., Sezerman, O. U., and Seidl-Seiboth, V. 2015. Molecular diversity of LysM
 563 carbohydrate-binding motifs in fungi. *Curr. Genet*. 61:103–113
- 564 Andersen, N. H., Cao, B., Rodríguez-Romero, A., and Arreguin, B. 1993. Hevein: NMR Assignment and
 565 Assessment of Solution-State Folding for the Agglutinin-Toxin Motif. *Biochemistry*. 32:1407–1422
- 566 Arnold, K., Bordoli, L., Kopp, J., and Schwede, T. 2006. The SWISS-MODEL workspace: a web-based
 567 environment for protein structure homology modelling. *Bioinformatics*. 22:195–201
- 568 Asensio, J. L., Cañada, F. J., Siebert, H.-C., Laynez, J., Poveda, A., Nieto, P. M., Soedjanaamadja, U.,
 569 Gabius, H.-J., and Jiménez-Barbero, J. 2000. Structural basis for chitin recognition by defense
 570 proteins: GlcNAc residues are bound in a multivalent fashion by extended binding sites in hevein

- 571 domains. *Chem. Biol.* 7:529–543
- 572 Böhm, H., Albert, I., Fan, L., Reinhard, A. A., and Nürnberger, T. 2014. Immune receptor complexes at the
573 plant cell surface. *Curr. Opin. Plant Biol.* 20:47–54
- 574 Bohne, A., Lang, E., and von der Lieth, C.-W. 1998. W3-SWEET: Carbohydrate Modeling By Internet. *J.*
575 *Mol. Model.* 4:33–43
- 576 Bohne, A., Lang, E., and von der Lieth, C. W. 1999. SWEET - WWW-based rapid 3D construction of oligo-
577 and polysaccharides. *Bioinformatics.* 15:767–768
- 578 Boller, T., and Felix, G. 2009. A renaissance of elicitors: perception of microbe-associated molecular
579 patterns and danger signals by pattern-recognition receptors. *Annu. Rev. Plant Biol.* 60:379–406
- 580 Bolton, M. D., Van Esse, H. P., Vossen, J. H., De Jonge, R., Stergiopoulos, I., Stulemeijer, I. J. E., Van Den
581 Berg, G. C. M., Borrás-Hidalgo, O., Dekker, H. L., De Koster, C. G., De Wit, P. J. G. M., Joosten, M. H.
582 A. J., and Thomma, B. P. H. J. 2008. The novel *Cladosporium fulvum* lysin motif effector Ecp6 is a
583 virulence factor with orthologues in other fungal species. *Mol. Microbiol.* 69:119–136
- 584 van den Burg, H. A., Harrison, S. J., Joosten, M. H. A. J., Vervoort, J., and de Wit, P. J. G. M. 2007.
585 *Cladosporium fulvum* Avr4 Protects Fungal Cell Walls Against Hydrolysis by Plant Chitinases
586 Accumulating During Infection. *Mol. Plant-Microbe Interact.* 19:1420–1430
- 587 Van Den Burg, H. A., Spronk, C. A. E. M., Boeren, S., Kennedy, M. A., Vissers, J. P. C., Vuister, G. W., De
588 Wit, P. J. G. M., and Vervoort, J. 2004. Binding of the AVR4 elicitor of *Cladosporium fulvum* to
589 chitotriose units is facilitated by positive allosteric protein-protein interactions: The chitin-binding
590 site of AVR4 represents a novel binding site on the folding scaffold shared between the inverte. *J.*
591 *Biol. Chem.* 279:16786–16796
- 592 Cao, Y., Liang, Y., Tanaka, K., Nguyen, C. T., Jedrzejczak, R. P., Joachimiak, A., and Stacey, G. 2014. The
593 kinase LYK5 is a major chitin receptor in *Arabidopsis* and forms a chitin-induced complex with
594 related kinase CERK1. *Elife.* 3
- 595 Cregeen, S., Radišek, S., Mandelc, S., Turk, B., Štajner, N., Jakše, J., and Javornik, B. 2015. Different Gene
596 Expressions of Resistant and Susceptible Hop Cultivars in Response to Infection with a Highly
597 Aggressive Strain of *Verticillium albo-atrum*. *Plant Mol. Biol. Report.* 33:689–704
- 598 Dawson, N. L., Sillitoe, I., Lees, J. G., Lam, S. D., and Orengo, C. A. 2017. CATH-Gene3D: Generation of the
599 resource and its use in obtaining structural and functional annotations for protein sequences. Pages
600 79–110 in: *Protein Bioinformatics. Methods in Molecular Biology*
- 601 Dodds, P. N., and Rathjen, J. P. 2010. Plant immunity: Towards an integrated view of plant–pathogen
602 interactions. *Nat. Rev. Genet.* 11:539–548
- 603 Duan, Y., Wu, C., Chowdhury, S., Lee, M. C., Xiong, G., Zhang, W., Yang, R., Cieplak, P., Luo, R., Lee, T.,
604 Caldwell, J., Wang, J., and Kollman, P. 2003. A point-charge force field for molecular mechanics
605 simulations of proteins based on condensed-phase quantum mechanical calculations. *J. Comput.*
606 *Chem.* 24:1999–2012
- 607 van Esse, H. P., Bolton, M. D., Stergiopoulos, I., de Wit, P. J. G. M., and Thomma, B. P. H. J. 2007. The
608 Chitin-Binding *Cladosporium fulvum* Effector Protein Avr4 Is a Virulence Factor. *Mol. Plant-Microbe*

- 609 Interact. 20:1092–1101
- 610 Finn, R. D., Bateman, A., Clements, J., Coggill, P., Eberhardt, R. Y., Eddy, S. R., Heger, A., Hetherington, K.,
611 Holm, L., Mistry, J., Sonnhammer, E. L. L., Tate, J., and Punta, M. 2014. Pfam: The protein families
612 database. *Nucleic Acids Res.* 42:222–230
- 613 Flajšman, M., Mandelc, S., Radišek, S., and Javornik, B. 2018. Xylem Sap Extraction Method from Hop
614 Plants. *BIO-PROTOCOL.* 7:1–11
- 615 Flajšman, M., Mandelc, S., Radišek, S., Štajner, N. N., Jakše, J., Košmelj, K., and Javornik, B. 2016.
616 Identification of Novel Virulence-Associated Proteins Secreted to Xylem by *Verticillium nonalfalfae*
617 During Colonization of Hop Plants. 29:362–373
- 618 Flajšman, M., Radišek, S., and Javornik, B. 2017. Pathogenicity Assay of *Verticillium nonalfalfae* on Hop
619 Plants. *BIO-PROTOCOL.* 7:1–10
- 620 Gubaeva, E., Gubaev, A., Melcher, R. L. J., Cord-Landwehr, S., Singh, R., El Gueddari, N. E., and
621 Moerschbacher, B. M. 2018. ‘Slipped Sandwich’ Model for Chitin and Chitosan Perception in
622 *Arabidopsis*. *Mol. Plant-Microbe Interact.* 31:1145–1153
- 623 Guillén, D., Sánchez, S., and Rodríguez-Sanoja, R. 2010. Carbohydrate-binding domains: multiplicity of
624 biological roles. *Appl. Microbiol. Biotechnol.* 85:1241–1249
- 625 Gust, A. A., Willmann, R., Desaki, Y., Grabherr, H. M., and Nürnberger, T. 2012. Plant LysM proteins:
626 modules mediating symbiosis and immunity. *Trends Plant Sci.* 17:495–502
- 627 Hayafune, M., Berisio, R., Marchetti, R., Silipo, A., Kayama, M., Desaki, Y., Arima, S., Squeglia, F.,
628 Ruggiero, A., Tokuyasu, K., Molinaro, A., Kaku, H., and Shibuya, N. 2014. Chitin-induced activation of
629 immune signaling by the rice receptor CEBiP relies on a unique sandwich-type dimerization. *Proc.*
630 *Natl. Acad. Sci.* 111:E404–E413
- 631 Hurlburt, N. K., Chen, L.-H., Stergiopoulos, I., and Fisher, A. J. 2018. Structure of the *Cladosporium fulvum*
632 *Avr4* effector in complex with (GlcNAc)₆ reveals the ligand-binding mechanism and uncouples its
633 intrinsic function from recognition by the Cf-4 resistance protein Y. Wang, ed. *PLOS Pathog.*
634 14:e1007263
- 635 Jakše, J., Čerenak, A., Radišek, S., Satovic, Z., Luthar, Z., and Javornik, B. 2013. Identification of
636 quantitative trait loci for resistance to *Verticillium* wilt and yield parameters in hop (*Humulus*
637 *lupulus* L.). *Theor. Appl. Genet.* 126:1431–1443
- 638 Jakše, J., Jelen, V., Radišek, S., de Jonge, R., Mandelc, S., Majer, A., Curk, T., Zupan, B., Thomma, B. P. H.
639 J., and Javornik, B. 2018. Genome sequence of xylem-invading *Verticillium nonalfalfae* lethal strain.
640 *Genome Announc.* 6:e01458-17
- 641 Jiménez-Barbero, J., Javier Cañada, F., Asensio, J. L., Aboitiz, N., Vidal, P., Canales, A., Groves, P., Gabius,
642 H.-J., and Siebert, H.-C. 2006. Hevein Domains: An Attractive Model to Study Carbohydrate–Protein
643 Interactions at Atomic Resolution. *Adv. Carbohydr. Chem. Biochem.* 60:303–354
- 644 Jones, J. D. G. G., and Dangl, J. L. 2006. The plant immune system. *Nature.* 444:323–329
- 645 de Jonge, R., van Esse, H. P., Kombrink, A., Shinya, T., Desaki, Y., Bours, R., van der Krol, S., Shibuya, N.,
646 Joosten, M. H. A. J., and Thomma, B. P. H. J. 2010. Conserved fungal LysM effector Ecp6 prevents

- 647 chitin-triggered immunity in plants. *Science*. 329:953–955
- 648 de Jonge, R., and Thomma, B. P. H. J. 2009. Fungal LysM effectors: extinguishers of host immunity?
649 *Trends Microbiol.* 17:151–157
- 650 Kastritis, P. L., and Bonvin, A. M. J. J. 2013. On the binding affinity of macromolecular interactions: Daring
651 to ask why proteins interact. *J. R. Soc. Interface.* 10:20120835
- 652 Kombrink, A., Rovenich, H., Shi-Kunne, X., Rojas-Padilla, E., van den Berg, G. C. M., Domazakis, E., de
653 Jonge, R., Valkenburg, D. J., Sanchez-Vallet, A., Seidl, M. F., and Thomma, B. P. H. J. 2017.
654 *Verticillium dahliae* LysM effectors differentially contribute to virulence on plant hosts. *Mol. Plant*
655 *Pathol.* 18:596–608
- 656 Krieger, E., and Vriend, G. 2015. New ways to boost molecular dynamics simulations. *J. Comput. Chem.*
657 36:996–1007
- 658 Krieger, E., and Vriend, G. 2014. YASARA View - molecular graphics for all devices - from smartphones to
659 workstations. *Bioinformatics.* 30:2981–2982
- 660 Langezaal, C. R., and Scheffer, J. J. C. 1992. Initiation and growth characterization of some hop cell
661 suspension cultures. *Plant Cell. Tissue Organ Cult.* 30:159–164
- 662 Lerner, D. R., and Raikhel, N. V. 1992. The gene for stinging nettle lectin (*Urtica dioica* agglutinin)
663 encodes both a lectin and a chitinase. *J. Biol. Chem.* 267:11085–11091
- 664 Li, W., Cowley, A., Uludag, M., Gur, T., McWilliam, H., Squizzato, S., Park, Y. M., Buso, N., and Lopez, R.
665 2015. The EMBL-EBI bioinformatics web and programmatic tools framework. *Nucleic Acids Res.*
666 43:W580–W584
- 667 Liu, P., and Stajich, J. E. 2015. Characterization of the Carbohydrate Binding Module 18 gene family in the
668 amphibian pathogen *Batrachochytrium dendrobatidis*. *Fungal Genet. Biol.* 77:31–39
- 669 Liu, S., Wang, J., Han, Z., Gong, X., Zhang, H., and Chai, J. 2016. Molecular Mechanism for Fungal Cell Wall
670 Recognition by Rice Chitin Receptor OsCEBiP. *Structure.* 24:1192–1200
- 671 Liu, T., Liu, Z., Song, C., Hu, Y., Han, Z., She, J., Fan, G., Wang, J., Jin, C., Chang, J., Zhou, J. M., and Chai, J.
672 2012. Chitin-induced dimerization activates a plant immune receptor. *Science.* 336:1160–1164
- 673 Liu, W., Xie, Y., Ma, J., Luo, X., Nie, P., Zuo, Z., Lahrmann, U., Zhao, Q., Zheng, Y., Zhao, Y., Xue, Y., and
674 Ren, J. 2015. IBS: an illustrator for the presentation and visualization of biological sequences.
675 *Bioinformatics.* 31:3359–61
- 676 Lombard, V., Golaconda Ramulu, H., Drula, E., Coutinho, P. M., and Henrissat, B. 2014. The carbohydrate-
677 active enzymes database (CAZy) in 2013. *Nucleic Acids Res.* 42:D490-495
- 678 Macho, A. P., and Zipfel, C. 2014. Plant PRRs and the activation of innate immune signaling. *Mol. Cell.*
679 54:263–272
- 680 Mandelc, S., and Javornik, B. 2015. The secretome of vascular wilt pathogen *Verticillium albo-atrum* in
681 simulated xylem fluid. *Proteomics.* 15:787–797
- 682 Marshall, R., Kombrink, A., Motteram, J., Loza-Reyes, E., Lucas, J., Hammond-Kosack, K. E., Thomma, B. P.

- 683 H. J., and Rudd, J. J. 2011. Analysis of Two in Planta Expressed LysM Effector Homologs from the
684 Fungus *Mycosphaerella graminicola* Reveals Novel Functional Properties and Varying Contributions
685 to Virulence on Wheat. *PLANT Physiol.* 156:756–769
- 686 Marton, K., Flajšman, M., Radišek, S., Košmelj, K., Jakše, J., Javornik, B., and Berne, S. 2018.
687 Comprehensive analysis of *Verticillium nonalfalfae* in silico secretome uncovers putative effector
688 proteins expressed during hop invasion. *PLoS One.* 13:e0198971
- 689 Mentlak, T., Kombrink, A., Shinya, T., Ryder, L. S., Otomo, I., Saitoh, H., Terauchi, R., Nishizawa, Y.,
690 Shibuya, N., Thomma, B. P. H. J., and Talbot, N. J. 2012. Effector-Mediated Suppression of Chitin-
691 Triggered Immunity by *Magnaporthe oryzae* Is Necessary for Rice Blast Disease. *Plant Cell.* 24:322–
692 335
- 693 Miya, A., Albert, P., Shinya, T., Desaki, Y., Ichimura, K., Shirasu, K., Narusaka, Y., Kawakami, N., Kaku, H.,
694 and Shibuya, N. 2007. CERK1, a LysM receptor kinase, is essential for chitin elicitor signaling in
695 *Arabidopsis*. *Proc. Natl. Acad. Sci.* 104:19613–19618
- 696 Mochizuki, S., Saitoh, K. ichiro, Minami, E., and Nishizawa, Y. 2011. Localization of probe-accessible chitin
697 and characterization of genes encoding chitin-binding domains during rice-*Magnaporthe oryzae*
698 interactions. *J. Gen. Plant Pathol.* 77:163–173
- 699 Möller, E. M. M., Bahnweg, G., Sandermann, H., and Geiger, H. H. H. 1992. A simple and efficient
700 protocol for isolation of high molecular weight DNA from filamentous fungi, fruit bodies, and
701 infected plant tissues. *Nucleic Acids Res.* 20:6115–6116
- 702 Progar, V., Jakše, J., Štajner, N., Radišek, S., Javornik, B., and Berne, S. 2017. Comparative transcriptional
703 analysis of hop responses to infection with *Verticillium nonalfalfae*. *Plant Cell Rep.* 36:1599–1613
- 704 Punja, Z. K., and Zhang, Y.-Y. 1993. Plant chitinases and their roles in resistance to fungal diseases. *J.*
705 *Nematol.* 25:526–540
- 706 Pusztahelyi, T. 2018. Chitin and chitin-related compounds in plant-fungal interactions. *Mycology.* 9:189–
707 201
- 708 Qi, X., Sun, Y., and Xiong, S. 2015. A single freeze-thawing cycle for highly efficient solubilization of
709 inclusion body proteins and its refolding into bioactive form. *Microb. Cell Fact.* 14:1–12
- 710 R Core Team. 2016. R: A Language and Environment for Statistical Computing.
- 711 Radišek, S., Jakše, J., and Javornik, B. 2004. Development of pathotype-specific SCAR markers for
712 detection of *Verticillium albo-atrum* isolates from hop. *Plant Dis.* 88:1115–1122
- 713 Radišek, S., Jakše, J., and Javornik, B. 2006. Genetic variability and virulence among *Verticillium albo-*
714 *atrum* isolates from hop. *Eur. J. Plant Pathol.* 116:301–314
- 715 Radišek, S., Jakše, J., Simončič, A., and Javornik, B. B. 2003. Characterization of *Verticillium albo-atrum*
716 Field Isolates Using Pathogenicity Data and AFLP Analysis. *Plant Dis.* 87:633–638
- 717 Ranf, S. 2017. Sensing of molecular patterns through cell surface immune receptors. *Curr. Opin. Plant*
718 *Biol.* 38:68–77
- 719 Sanchez-Vallet, A., Mesters, J. R., and Thomma, B. P. H. J. 2014. The battle for chitin recognition in plant-

- 720 microbe interactions. *FEMS Microbiol. Rev.* 39:171–183
- 721 Sanchez-Vallet, A., Saleem-Batcha, R., Kombrink, A., Hansen, G., Valkenburg, D.-J. J., Thomma, B. P. H. J.,
722 and Mesters, J. R. 2013. Fungal effector Ecp6 outcompetes host immune receptor for chitin binding
723 through intrachain LysM dimerization. *Elife.* 2013:1–16
- 724 Schmittgen, T. D., and Livak, K. J. 2008. Analyzing real-time PCR data by the comparative C(T) method.
725 *Nat. Protoc.* 3:1101–1108
- 726 Seidl, M. F., Faino, L., Shi-Kunne, X., van den Berg, G. C. M., Bolton, M. D., and Thomma, B. P. H. J. 2015.
727 The Genome of the Saprophytic Fungus *Verticillium tricorpus* Reveals a Complex Effector Repertoire
728 Resembling That of Its Pathogenic Relatives. *Mol. Plant-Microbe Interact.* 28:362–373
- 729 Shibuya, N., and Minami, E. 2001. Oligosaccharide signalling for defence responses in plant. *Physiol. Mol.*
730 *Plant Pathol.* 59:223–233
- 731 Shimizu, T., Nakano, T., Takamizawa, D., Desaki, Y., Ishii-Minami, N., Nishizawa, Y., Minami, E., Okada, K.,
732 Yamane, H., Kaku, H., and Shibuya, N. 2010. Two LysM receptor molecules, CEBiP and OsCERK1,
733 cooperatively regulate chitin elicitor signaling in rice. *Plant J.* 64:204–214
- 734 Shinya, T., Nakagawa, T., Kaku, H., and Shibuya, N. 2015. Chitin-mediated plant–fungal interactions:
735 catching, hiding and handshaking. *Curr. Opin. Plant Biol.* 26:64–71
- 736 Signorell, A. 2017. DescTools v0.99.19. Available at:
737 <https://www.rdocumentation.org/packages/DescTools/versions/0.99.19>.
- 738 Soanes, D. M., Alam, I., Cornell, M., Wong, H. M., Hedeler, C., Paton, N. W., Rattray, M., Hubbard, S. J.,
739 Oliver, S. G., and Talbot, N. J. 2008. Comparative genome analysis of filamentous fungi reveals gene
740 family expansions associated with fungal pathogenesis. *PLoS One.* 3:e2300
- 741 Sperschneider, J., Dodds, P. N., Singh, K. B., and Taylor, J. M. 2018. ApoplastP: prediction of effectors and
742 plant proteins in the apoplast using machine learning. *New Phytol.* 217:1764–1778
- 743 Štajner, N., Cregeen, S., and Javornik, B. 2013. Evaluation of Reference Genes for RT-qPCR Expression
744 Studies in Hop (*Humulus lupulus* L.) during Infection with Vascular Pathogen *Verticillium albo-*
745 *atrum*. *PLoS One.* 8:e68228
- 746 Stergiopoulos, I., van den Burg, H. A., Okmen, B., Beenen, H. G., van Liere, S., Kema, G. H. J., and de Wit,
747 P. J. G. M. 2010. Tomato Cf resistance proteins mediate recognition of cognate homologous
748 effectors from fungi pathogenic on dicots and monocots. *Proc. Natl. Acad. Sci.* 107:7610–7615
- 749 Stergiopoulos, I., De Kock, M. J. D., Lindhout, P., and De Wit, P. J. G. M. 2007. Allelic variation in the
750 effector genes of the tomato pathogen *Cladosporium fulvum* reveals different modes of adaptive
751 evolution. *Mol. Plant. Microbe. Interact.* 20:1271–1283
- 752 Takahara, H., Hacquard, S., Kombrink, A., Hughes, H. B., Halder, V., Robin, G. P., Hiruma, K., Neumann, U.,
753 Shinya, T., Kombrink, E., Shibuya, N., Thomma, B. P. H. J., O'Connell, R. J., and Connell, R. J. O. 2016.
754 *Colletotrichum higginsianum* extracellular LysM proteins play dual roles in appressorial function
755 and suppression of chitin-triggered plant immunity. *New Phytol.* 211:1323–1337
- 756 Trott, O., and Olson, A. J. 2010. Software news and update AutoDock Vina: Improving the speed and
757 accuracy of docking with a new scoring function, efficient optimization, and multithreading. *J.*

758 Comput. Chem. 31:455–461

759 Waterhouse, A., Bertoni, M., Bienert, S., Studer, G., Tauriello, G., Gumienny, R., Heer, F. T., de Beer, T. A.
760 P., Rempfer, C., Bordoli, L., Lepore, R., and Schwede, T. 2018. SWISS-MODEL: homology modelling
761 of protein structures and complexes. *Nucleic Acids Res.* 46:W296–W303

762 Wright, H. T., Sandrasegaram, G., and Wright, C. S. 1991. Evolution of a family of N-acetylglucosamine
763 binding proteins containing the disulfide-rich domain of wheat germ agglutinin. *J. Mol. Evol.*
764 33:283–294

765

766 **Tables**

767 **Table 1.** Comparison of chitin oligomer binding affinities of various fungal effectors and plant defense
 768 proteins, obtained using ITC or SPR. The proteins are organized according to binding affinity.

Organism	Protein	CAZy	Ligand	K _d (μM)	Method	Reference
<i>FUNGUS</i>						
<i>Cladosporium fulvum</i>	Ecp6	CBM50	(GlcNAc) ₆	2.8 × 10 ⁻⁴ , ^a 1.7	ITC	(Sanchez-Vallet et al. 2013)
<i>Colletotrichum higginsianum</i>	ChELP1	CBM50	(GlcNAc) ₈ -Bio	2.6 × 10 ⁻⁵	SPR	(Takahara et al. 2016)
<i>Colletotrichum higginsianum</i>	ChELP2	CBM50	(GlcNAc) ₈ -Bio	2.5 × 10 ⁻⁴	SPR	(Takahara et al. 2016)
<i>Cladosporium fulvum</i>	Ecp6	CBM50	(GlcNAc) ₈	1.3 × 10 ⁻³	SPR	(Mentlak et al. 2012)
<i>Magnaporthe oryzae</i>	Slp1	CBM50	(GlcNAc) ₈	2.4 × 10 ⁻³	SPR	(Mentlak et al. 2012)
<i>Verticillium nonalfalfae</i>	VnaChtBP	CBM18	(GlcNAc) ₆	0.78 ± 0.58	SPR	This study
<i>Cladosporium fulvum</i>	Avr4	CBM14	(GlcNAc) ₆	6.3 ± 0.23	ITC	(Van Den Burg et al. 2004)
<i>Cladosporium fulvum</i>	Ecp6	CBM50	(GlcNAc) _{4,5,6,8}	11.5 to 3.7	ITC	(de Jonge et al. 2010)
<i>PLANT</i>						
<i>Arabidopsis thaliana</i>	AtLYK5	CBM50	(GlcNAc) ₈	1.72	ITC	(Cao et al. 2014)
<i>Hevea brasiliensis</i>	Hevein	CBM18	(GlcNAc) ₅	2.1	ITC	(Asensio et al. 2000)
<i>Arabidopsis thaliana</i>	AtCERK1	CBM50	(GlcNAc) ₈	455	ITC	(Cao et al. 2014)
<i>Arabidopsis thaliana</i>	AtCERK1	CBM50	(GlcNAc) ₈	448	ITC	(Liu et al. 2012)

769 ITC, isothermal titration calorimetry; SPR, surface plasmon resonance, CBM, carbohydrate-binding module; GlcNAc,
 770 N-Acetylglucosamin; Bio, biotinylated; ^a Ecp6 displays biphasic binding of chitin hexamer in pM range to LysM1-
 771 LysM3 groove and in μM range to LysM2 domain.

772 **Table 2.** The results of homology modelling of the VnaChtBP using the SWISS-MODEL server.

	Template	Description	Seq Identity	Oligo-States	GMOE	QMEAN	Coverage
Model01	2uwg.1.A	Wheat germ lectin	43.98%	Homo-dimer	0.31	-4.61	98-318
Model02	2wgc.1.A	Agglutin isolectin 1	40.96%	Homo-dimer	0.32	-3.22	39-254
Model03	1ulk.1.A	Lectin-C	49.15%	Homo-dimer	0.20	-0.65	212-378

773

774 **Figure captions**

775 **Fig. 1.** Domain architecture (A-D) and gene expression (E) of CBM18-containing proteins identified in
 776 *Verticillium nonalfalfae*. Protein organization was determined by querying protein sequences against
 777 CATH-Gene3D (Dawson et al. 2017) using the FunFHMMer web server and presented by IBS software
 778 (Liu et al. 2015). Proteins were classified into four groups: Lectin-like proteins (A), Chitinases (B), Chitin
 779 deacetylases (C) and Xyloglucan endotransglucosylase (D). Gene expression is presented as a heatmap of
 780 \log_2 CPM values determined by RNA sequencing of infected hop (Progar et al. 2017).

781 **Fig. 2.** *VnaChtBP*, a gene encoding the CBM18 chitin binding protein of *Verticillium nonalfalfae*, is highly
 782 expressed in stems of susceptible hop at the late stages of infection. The gene expression of *VnaChtBP*
 783 was quantified by RT-qPCR using cDNA prepared from the roots and shoots of infected susceptible
 784 ('Celeia') and resistant ('Wye Target') hop plants (n = 5) at 6, 12 and 18 dpi and the expression levels
 785 were normalised relative to the expression of the gene in ½ liquid Czapek-Dox medium using
 786 topoisomerase (*VnaUn.148*) and splicing factor 3a2 (*Vna8.801*) as housekeeping genes (Marton et al.
 787 2018). One way ANOVA with Tukey's post hoc test was performed to test for differences between the
 788 group means. FC, fold change; dpi, days post inoculation.

789 **Fig. 3.** A carbohydrate sedimentation test confirmed that the recombinant protein VnaChtBP specifically
 790 binds to chitin. A recombinant protein (15 µg) that bound to chitin beads and crab shell chitin was
 791 detected in the sediment, and it was present in the supernatant when incubated with cellulose, xylan or
 792 without the addition of carbohydrates (control). Western blot analysis was performed with primary
 793 antibody His-probe (H-3) (SCBT) (1:1,000) and secondary chicken anti-mouse IgG-HRP (SCBT) (1:5,000).
 794 Protein bands were detected using Super Signal West Pico (ThermoFisher Scientific) ECL substrate in a
 795 GelDoc-It2 Imager (UVP).

796 **Fig. 4.** SPR analysis of chitin hexamer binding to VnaChtBP. Different concentrations (0.05, 0.1, 0.2, 0.4,
 797 0.8, 1.6, 3.2 and 6.4 µM) of (GlcNAc)₆ were tested for the binding (top panel). The binding curve (bottom
 798 panel) was generated by fitting steady state response levels at the end of the association phase, versus
 799 the concentration of the injected chitin hexamer. K_d was obtained by fitting the data to the steady-state
 800 affinity model. For reproducibility of binding, three independent titration experiments were performed.
 801 (GlcNAc)₆, hexa-N-acetyl chitohexaose

802 **Fig 5.** VnaChtBP protects fungus against degradation by plant chitinases. Micrographs of *Trichoderma*
 803 *viride* germinating spores, preincubated at RT for 2 h with 3 µM VnaChtBP, followed by the addition of
 804 xylem sap (19 U of chitinase/mg total protein) from *V. nonalfalfae* infected hop, were taken 24 h after
 805 treatment. The recombinant protein VnaChtBP caused aggregation and compaction of *T. viride* hyphae
 806 and protected the fungus from degradation by xylem sap chitinases. The chitinase activity of xylem sap
 807 was measured as a release of dye from Chitin Azure and one chitinase unit was defined as the amount of
 808 enzyme that caused a 0.01 increase in absorbance at 575 nm, measured at pH 5.0 and 25°C.

809 **Fig. 6.** VnaChtBP prevents chitin-induced activation of plant immune receptors. Reactive oxygen species
 810 (ROS) released from hop suspension cells in response to chitin hexamer (GlcNAc)₆ were measured using
 811 a chemiluminescent assay with 100 µM luminol-based substrate L-012 and 40 µg/ml horseradish

812 peroxidase. Generation of ROS was elicited with 1 μM $(\text{GlcNAc})_6$ in the absence and presence of 5 μM
 813 VnaChtBP or with 5 μM VnaChtBP for control. Data were background-corrected and presented as a
 814 median with 95% confidence interval of 5 measurements. The area under the curve of the chitin-treated
 815 group, VnaChtBP-treated group and the chitin plus VnaChtBP group were compared using a non-
 816 parametric Kruskal-Wallis test with Holm's post hoc analysis (p -value $< 2.2e^{-16}$).

817 **Fig. 7.** Confirmation of VnaChtBP dimerization (A), CD spectra of VnaChtBP in the absence and presence
 818 of chitin hexamer (B) and a schematic representation of the VnaChtBP homology model in complex with
 819 chitin hexamer (C). A: The effector gene *VnaChtBP* was cloned into the vectors pDEST22 and pDEST32 to
 820 serve as both bait and prey and yeast-two-hybrid assay was performed. Weak dimerization of the
 821 effector was confirmed on a triple dropout reporter media SC-LWH and no self-activation of the pDEST22
 822 construct with empty pDEST32 vector was detected on the X-gal reporter. B: CD spectra of 2.5 μM
 823 VnaChtBP in the absence and presence of 25 μM chitin hexamer ($(\text{GlcNAc})_6$) were recorded on a Jasco J-
 824 1500 CD spectrometer at 25 $^\circ\text{C}$ and pH 8.0. Binding of chitin hexamer to VnaChtBP induced additional
 825 secondary structure formation. C: The 3D model of VnaChtBP obtained by Swiss-Model (Arnold et al.
 826 2006; Waterhouse et al. 2018) was refined by YASARA Structure (Krieger and Vriend 2014, 2015) and
 827 used in YASARA's AutoDock VINA module (Trott and Olson 2010) for molecular docking of chitin
 828 hexamer, built in the SWEET PROGRAM (Bohne et al. 1998, 1999). VnaChtBP is in dimeric form, the
 829 chitin binding domains of the Chain A (Chain B) are in cyan (grey) color shades. The chitin hexamer is
 830 shown in stick representation.

831 **Fig. 8.** Symptom development (A) and disease severity index (DSI) assessment (B) in susceptible hop
 832 following infection with the wild type *V. nonalfalfae* and two knockout mutants of *VnaChtBP*. Plants of
 833 susceptible hop 'Celeia' were inoculated by root dipping in 5×10^6 conidia/ml suspension and *Verticillium*
 834 wilting symptoms were assessed five times post inoculation. A: Both *VnaChtBP* deletion mutants
 835 displayed *Verticillium* wilting symptoms (chlorosis and necrosis of the leaves) in susceptible hop similar
 836 to the wild type fungus. Pictures were taken 35 days post inoculation. B: According to the DSI assessment
 837 with a 0-5 scale (Radišek et al. 2003), there were no significant differences between the wild type *V.*
 838 *nonalfalfae* and knockout mutants of *VnaChtBP*. Means with SE were calculated for 10 plants per
 839 treatment. Dpi, days post inoculation.

840 **Supplementary Information**

841 **e-Xtra Table S1** lists *Verticillium* spp. isolates examined for the presence of *VnaChtBP*.

842 **e-Xtra Table S2** shows sequence conservation of the closest VnaChtBP homologs as determined by
 843 *blastp* analysis against the NCBI non-redundant database.

844 **e-Xtra Table S3** lists primers used for cloning, gene disruption and expression of VnaChtBP, fungal
 845 identification and relative biomass quantification.

846 **e-Xtra File S1** presents the results of *NCBI BLAST+* query with the VnaChtBP sequence against the
 847 UniProt Knowledgebase at Interpro, summarizing protein family and domain predictions of homologous
 848 proteins.

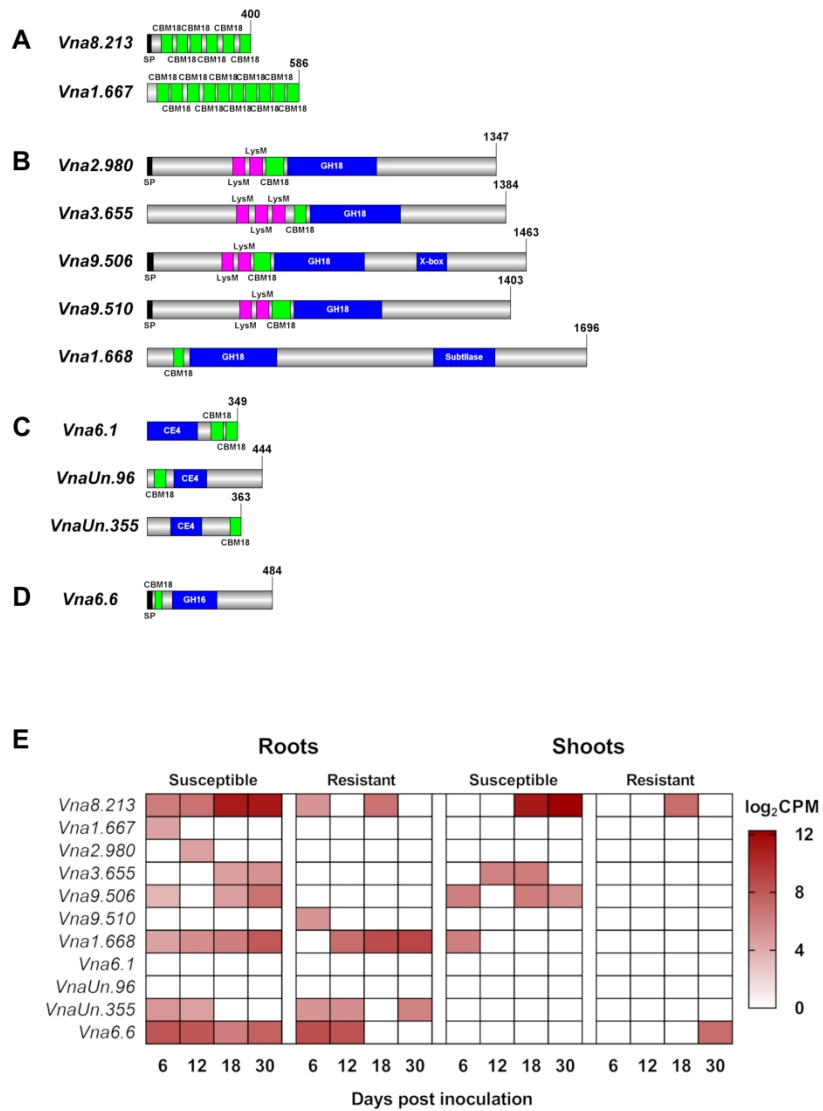
849 **e-Xtra File S2** contains the *Clustal O* nucleotide sequence alignment of the *V. nonalfalfae VnaChtBP*
850 gene, *V. alfalfae VaChtBP* gene and the corresponding translation to the amino acid sequence with
851 marked non-synonymous substitutions.

852 **e-Xtra Fig. S1** shows domain architecture and gene expression of likely LysM effector proteins identified
853 in *Verticillium nonalfalfae*. Protein organization was determined by matching protein sequences against
854 the InterPro protein signature databases using the InterProScan tool. Results were presented by IBS
855 software (Liu et al. 2015). Gene expression is presented as a heatmap of log₂CPM values determined by
856 RNA sequencing of infected hop (Progar et al. 2017).

857 **e-Xtra Fig. S2** presents SDS-PAGE and western blot analysis of recombinant VnaChtBP production.
858 Protein was expressed overnight at 16°C in *E. coli* SHuffle T7 cells (A), refolded from inclusion bodies (IB)
859 using a mild solubilization method (Qi et al. 2015) and Ni-NTA affinity purified (B). Protein samples were
860 separated by SDS-PAGE, transferred to a PVDF membrane and stained with Ponceau S. Western blot
861 analysis was performed with primary antibody His-probe (H-3) (SCBT) (1:1,000) and secondary Chicken
862 anti-mouse IgG-HRP (SCBT) (1:5,000). Protein bands were detected in the UVP gel imaging system using
863 ECL substrate. T, total proteins; S, supernatant; P, pellet

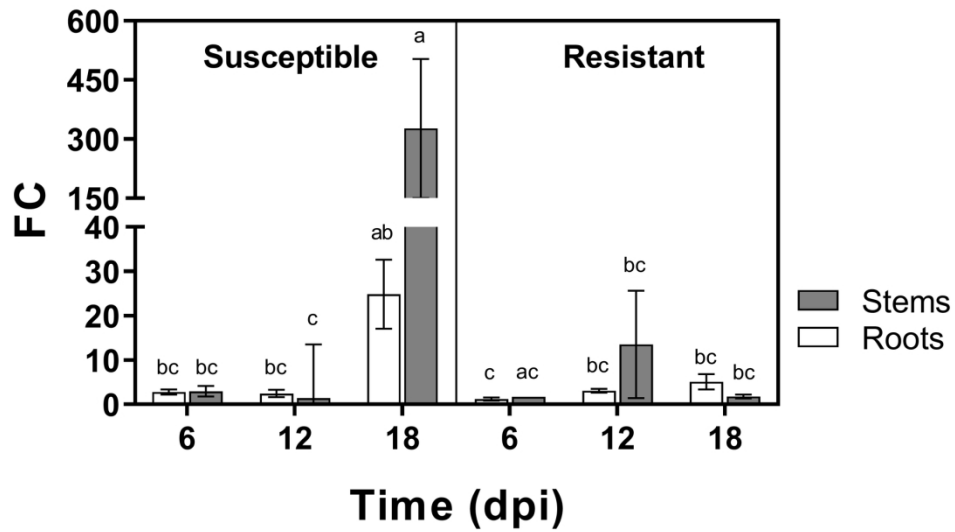
864 **e-Xtra Fig. S3** shows binding of various carbohydrates to recombinant VnaChtBP. Protein (0.1 mg/ml)
865 was immobilized to the surface of a CM5 sensor chip and binding of N-acetyl glucosamine (NAG),
866 glucosamine (GlcN), glucose (Glc), galactose (Gal) and mannose (Man) at a 500 μM concentration in HBS
867 buffer (10 mM HEPES, 140 mM NaCl, pH 7.4) was monitored on Biacore T100.

868 **e-Xtra Fig. S4** presents the morphology, sporulation and infectivity of *Verticillium nonalfalfae* wild type
869 and *VnaChtBP* knockout mutants (A) and relative fungal biomass quantification in infected hop (B).
870 Sporulation assessment 5 denotes 100% conidiation, while 1 denotes 20% conidiation of the wild type.
871 Infectivity of 100% means all plants were infected with *V. nonalfalfae* as determined by fungal re-
872 isolation from infected hop. The relative quantity of *V. nonalfalfae* DNA in infected hop was estimated at
873 21 dpi with the 2^{-ΔΔCt} method (Schmittgen and Livak 2008) using *V. nonalfalfae* lethal genotype (PG2)
874 specific primer 5-1gs (Radišek et al. 2004) and hop reference gene DRH1 (DEAD box RNA helicase) for
875 normalization (Štajner et al. 2013). Amplification levels are expressed relative to those obtained from
876 plants infected with the wild type strain. One-way ANOVA with Tukey's multiple comparison test was
877 performed in GraphPad Prism 8.02 (GraphPad Software, San Diego, California USA, www.graphpad.com)
878 to test for difference between the wild type and mutant group means.



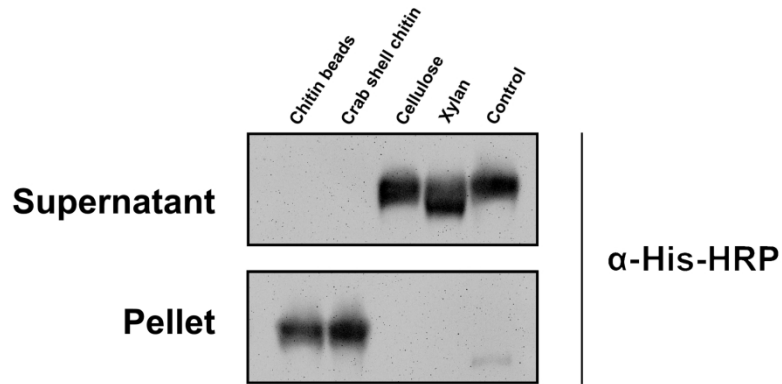
Domain architecture (A-D) and gene expression (E) of CBM18-containing proteins identified in *Verticillium nonalfalfae*. Protein organization was determined by querying protein sequences against CATH-Gene3D (Dawson et al. 2017) using the FunFHMmer web server and presented by IBS software (Liu et al. 2015). Proteins were classified into four groups: Lectin-like proteins (A), Chitinases (B), Chitin deacetylases (C) and Xyloglucan endotransglucosylase (D). Gene expression is presented as a heatmap of log₂CPM values determined by RNA sequencing of infected hop (Progar et al. 2017).

177x246mm (300 x 300 DPI)



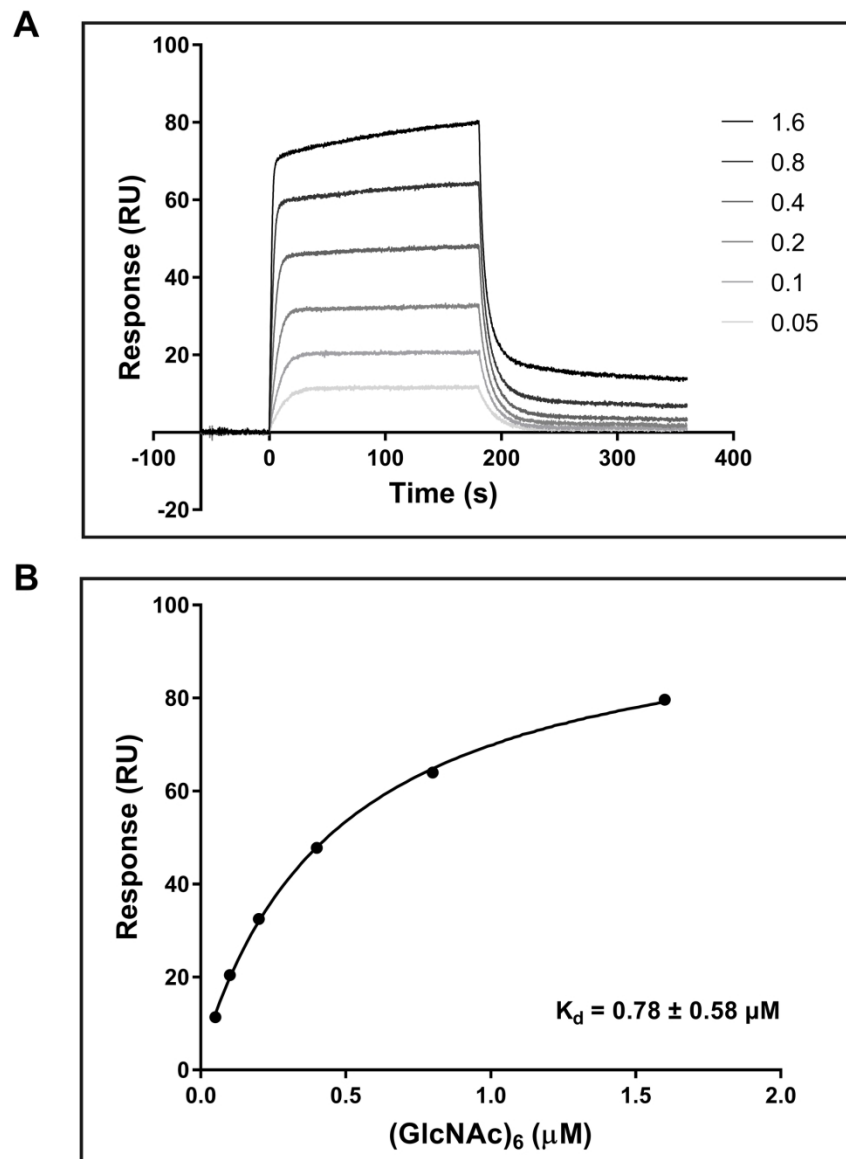
VnaChtBP, a gene encoding the CBM18 chitin binding protein of *Verticillium nonalfalae*, is highly expressed in stems of susceptible hop at the late stages of infection. The gene expression of *VnaChtBP* was quantified by RT-qPCR using cDNA prepared from the roots and shoots of infected susceptible ('Celeia') and resistant ('Wye Target') hop plants (n = 5) at 6, 12 and 18 dpi and the expression levels were normalised relative to the expression of the gene in ½ liquid Czapek-Dox medium using topoisomerase (*VnaUn.148*) and splicing factor 3a2 (*Vna8.801*) as housekeeping genes (Marton et al. 2018). One way ANOVA with Tukey's post hoc test was performed to test for differences between the group means. FC, fold change; dpi, days post inoculation.

170x101mm (300 x 300 DPI)



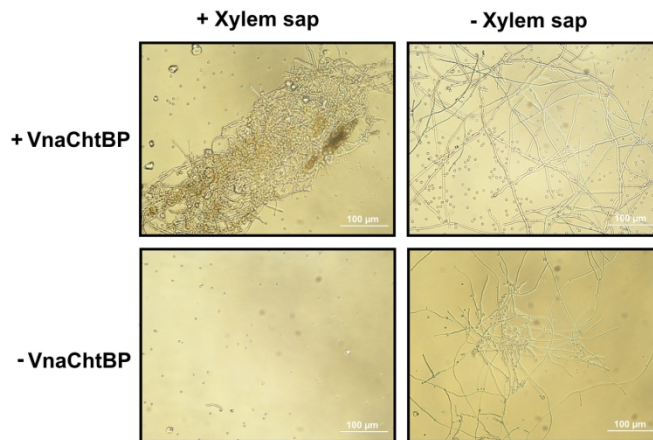
A carbohydrate sedimentation test confirmed that the recombinant protein VnaChtBP specifically binds to chitin. A recombinant protein (15 μg) that bound to chitin beads and crab shell chitin was detected in the sediment, and it was present in the supernatant when incubated with cellulose, xylan or without the addition of carbohydrates (control). Western blot analysis was performed with primary antibody His-probe (H-3) (SCBT) (1:1,000) and secondary chicken anti-mouse IgG-HRP (SCBT) (1:5,000). Protein bands were detected using Super Signal West Pico (ThermoFisher Scientific) ECL substrate in a GelDoc-It2 Imager (UVP).

215x101mm (300 x 300 DPI)



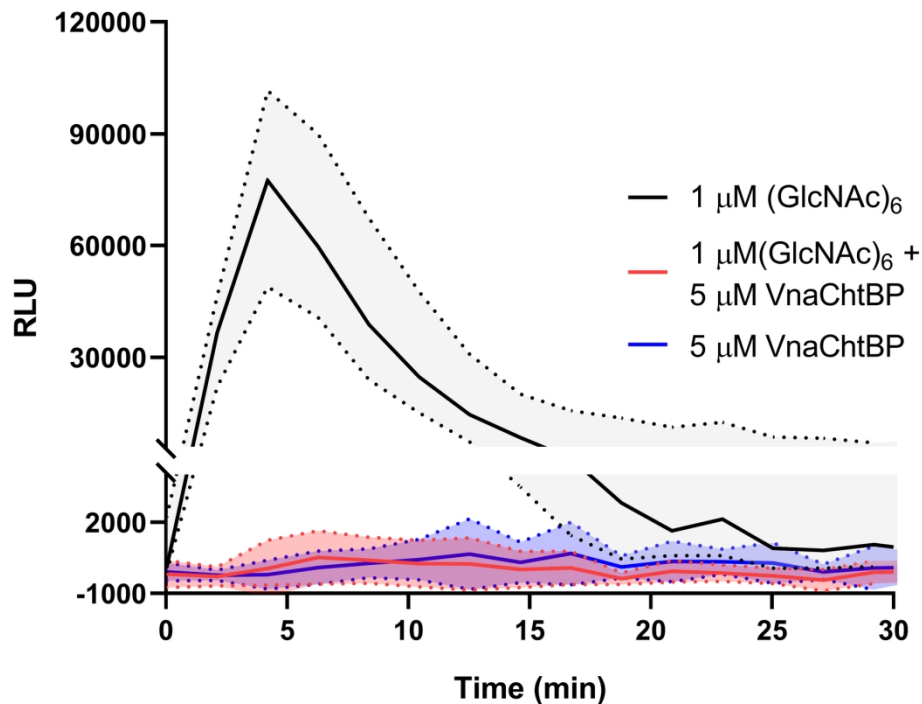
SPR analysis of chitin hexamer binding to VnaChtBP. Different concentrations (0.05, 0.1, 0.2, 0.4, 0.8, 1.6, 3.2 and 6.4 μM) of (GlcNAc)₆ were tested for the binding (top panel). The binding curve (bottom panel) was generated by fitting steady state response levels at the end of the association phase, versus the concentration of the injected chitin hexamer. K_d was obtained by fitting the data to the steady-state affinity model. For reproducibility of binding, three independent titration experiments were performed. (GlcNAc)₆, hexa-N-acetyl chitohexaose

177x244mm (300 x 300 DPI)



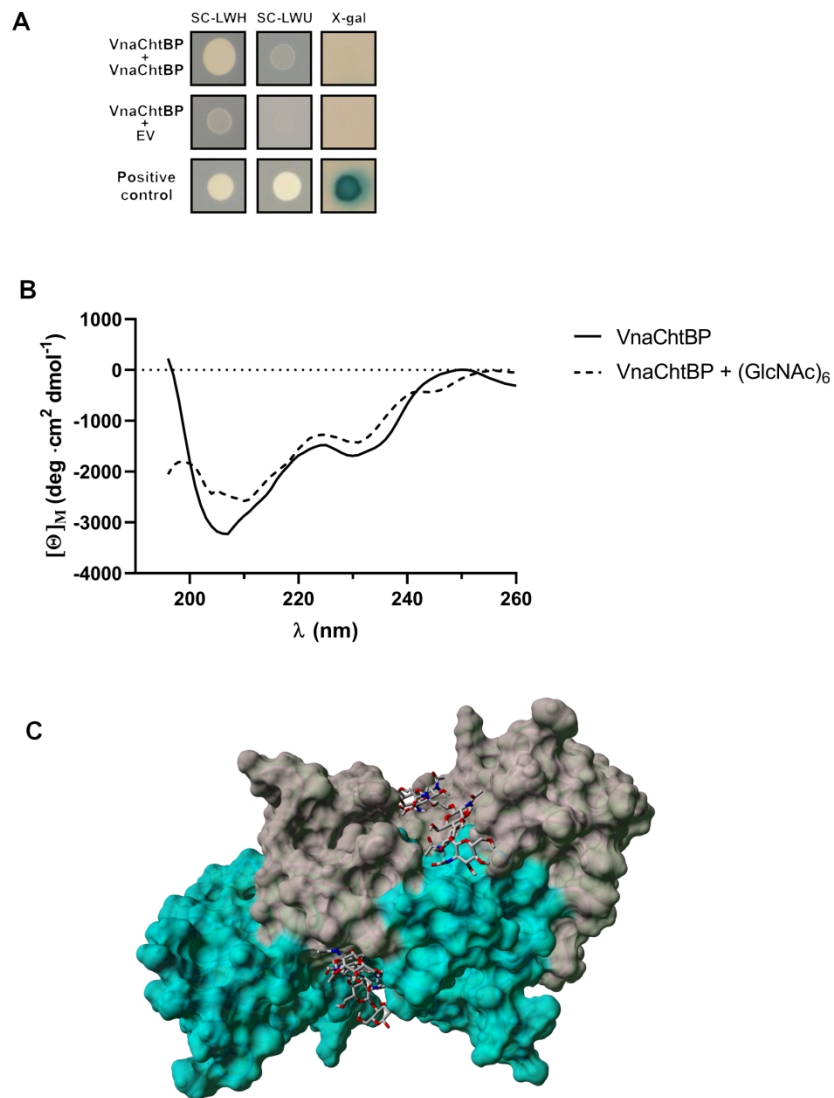
VnaChtBP protects fungus against degradation by plant chitinases. Micrographs of *Trichoderma viride* germinating spores, preincubated at RT for 2 h with 3 µM VnaChtBP, followed by the addition of xylem sap (19 U of chitinase/mg total protein) from *V. nonalfalae* infected hop, were taken 24 h after treatment. The recombinant protein VnaChtBP caused aggregation and compaction of *T. viride* hyphae and protected the fungus from degradation by xylem sap chitinases. The chitinase activity of xylem sap was measured as a release of dye from Chitin Azure and one chitinase unit was defined as the amount of enzyme that caused a 0.01 increase in absorbance at 575 nm, measured at pH 5.0 and 25°C.

177x94mm (300 x 300 DPI)



VnaChtBP prevents chitin-induced activation of plant immune receptors. Reactive oxygen species (ROS) released from hop suspension cells in response to chitin hexamer (GlcNAc)₆ were measured using a chemiluminescent assay with 100 μM luminol-based substrate L-012 and 40 μg/ml horseradish peroxidase. Generation of ROS was elicited with 1 μM (GlcNAc)₆ in the absence and presence of 5 μM VnaChtBP or with 5 μM VnaChtBP for control. Data were background-corrected and presented as a median with 95% confidence interval of 5 measurements. The area under the curve of the chitin-treated group, VnaChtBP-treated group and the chitin plus VnaChtBP group were compared using a non-parametric Kruskal-Wallis test with Holm's post hoc analysis (p-value < 2.2e⁻¹⁶).

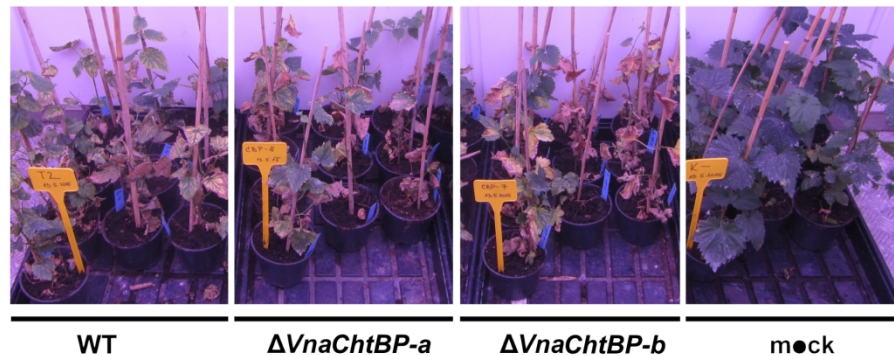
170x129mm (300 x 300 DPI)



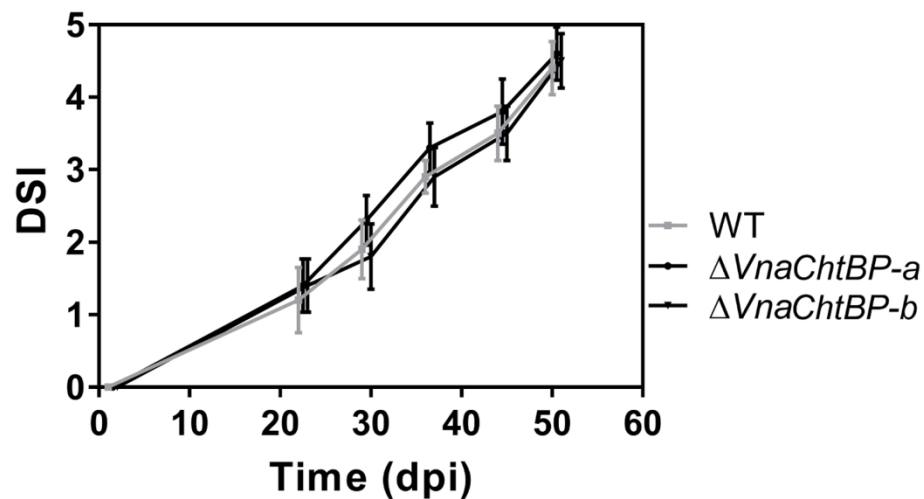
Confirmation of VnaChtBP dimerization (A), CD spectra of VnaChtBP in the absence and presence of chitin hexamer (B) and a schematic representation of the VnaChtBP homology model in complex with chitin hexamer (C). A: The effector gene VnaChtBP was cloned into the vectors pDEST22 and pDEST32 to serve as both bait and prey and yeast-two-hybrid assay was performed. Weak dimerization of the effector was confirmed on a triple dropout reporter media SC-LWH and no self-activation of the pDEST22 construct with empty pDEST32 vector was detected on the X-gal reporter. B: CD spectra of 2.5 μM VnaChtBP in the absence and presence of 25 μM chitin hexamer ((GlcNAc)₆) were recorded on a Jasco J-1500 CD spectrometer at 25 °C and pH 8.0. Binding of chitin hexamer to VnaChtBP induced additional secondary structure formation. C: The 3D model of VnaChtBP obtained by Swiss-Model (Arnold et al. 2006; Waterhouse et al. 2018) was refined by YASARA Structure (Krieger and Vriend 2014, 2015) and used in YASARA's AutoDock VINA module (Trott and Olson 2010) for molecular docking of chitin hexamer, built in the SWEET PROGRAM (Bohne et al. 1998, 1999). VnaChtBP is in dimeric form, the chitin binding domains of the Chain A (Chain B) are in cyan (grey) color shades. The chitin hexamer is shown in stick representation.

177x245mm (300 x 300 DPI)

A



B



Symptom development (A) and disease severity index (DSI) assessment (B) in susceptible hop following infection with the wild type *V. nonalfalae* and two knockout mutants of *VnaChtBP*. Plants of susceptible hop 'Celeia' were inoculated by root dipping in 5×10^6 conidia/ml suspension and Verticillium wilting symptoms were assessed five times post inoculation. A: Both *VnaChtBP* deletion mutants displayed Verticillium wilting symptoms (chlorosis and necrosis of the leaves) in susceptible hop similar to the wild type fungus. Pictures were taken 35 days post inoculation. B: According to the DSI assessment with a 0-5 scale (Radišek et al. 2003), there were no significant differences between the wild type *V. nonalfalae* and knockout mutants of *VnaChtBP*. Means with SE were calculated for 10 plants per treatment. Dpi, days post inoculation.

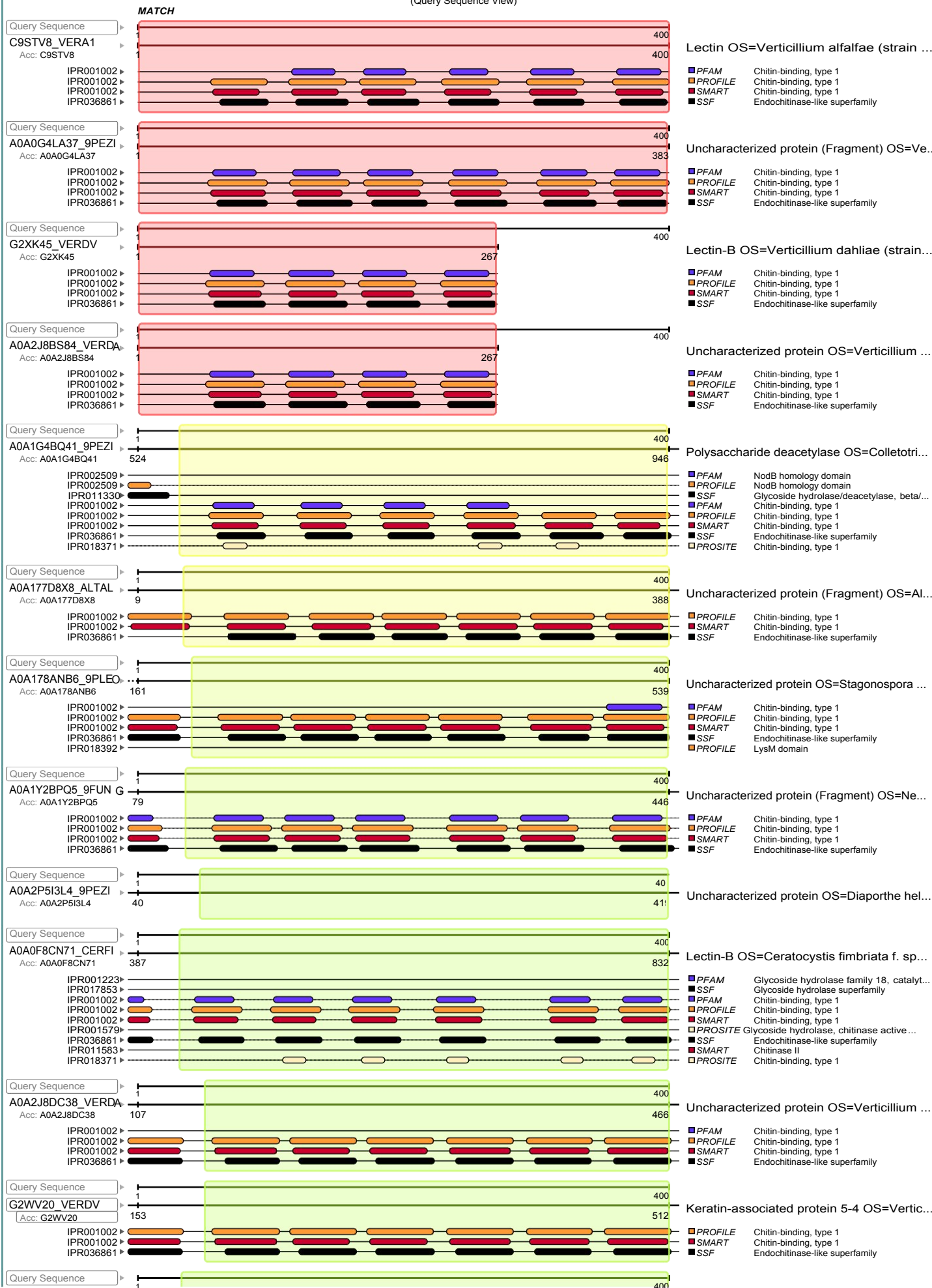
blastp (version: BLASTP 2.7.1+)

Database: uniprotkb
 Sequence: VNA8.2131-400
 Length: 400

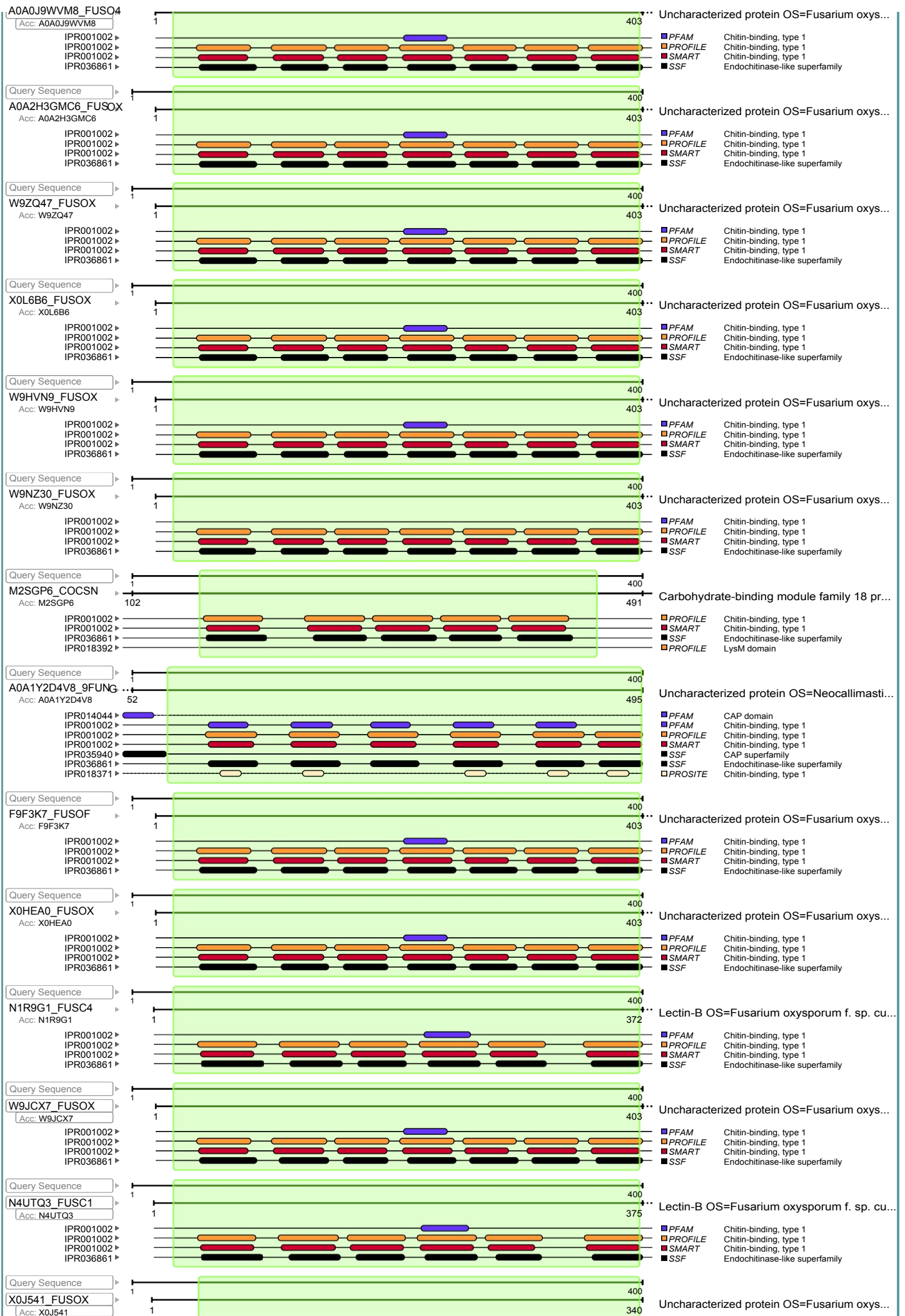
Sun, Jul 01, 2018 at 13:33:10

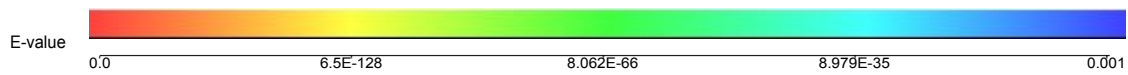
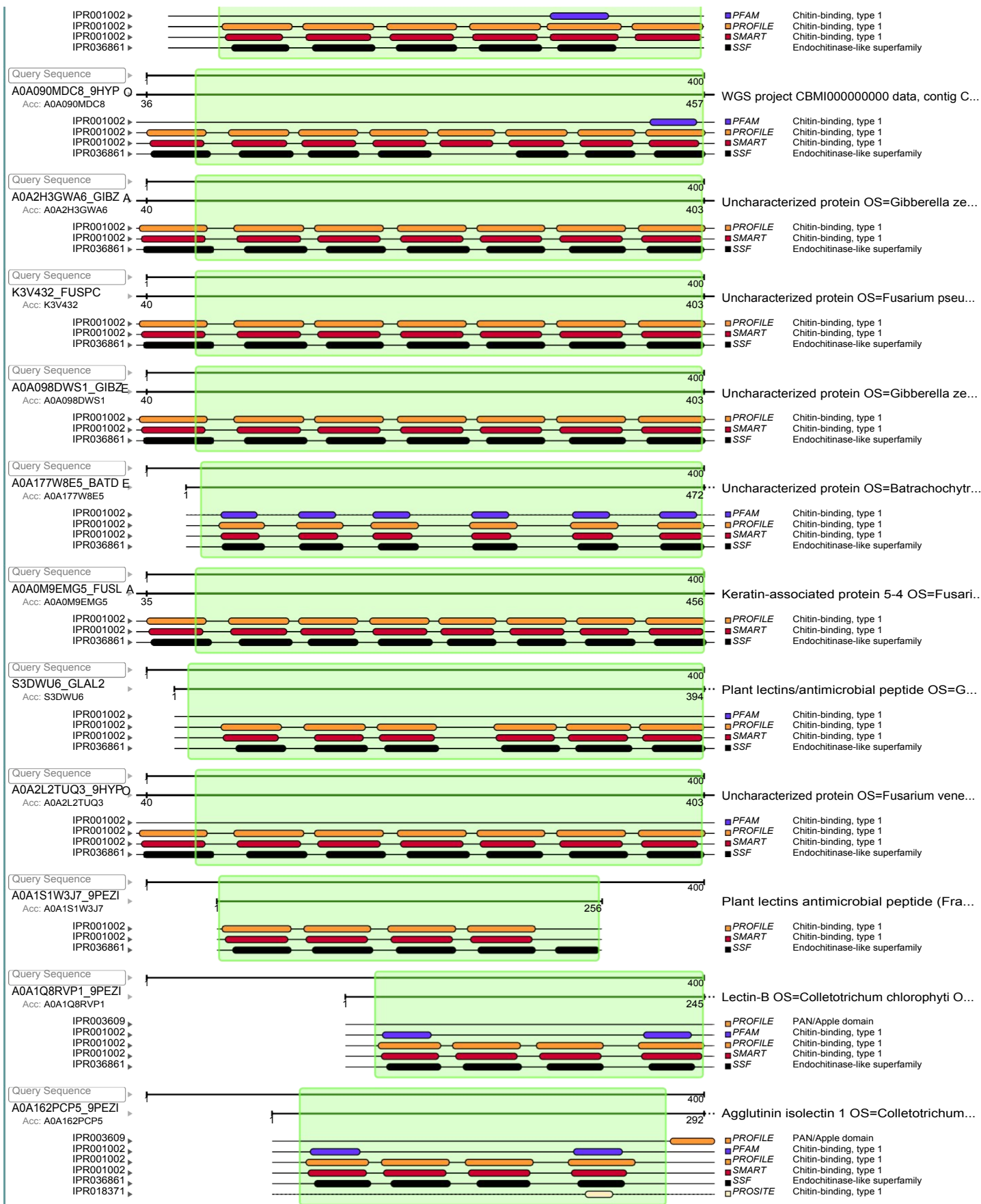
Sun, Jul 01, 2018 at 13:34:15

Fast Family and Domain Prediction
 (Query Sequence View)









CLUSTAL O(1.2.4) multiple sequence alignment

Vna: DNA sequence of *VnaChtBP* (MH325205)

Va: DNA sequence of *VaCBP* (MH325206)

P_Vna: protein sequence of *VnaChtBP*

Δ: amino-acid in the Va sequence that differs from Vna sequence

Underlined: SingalP

Grey: Chitin binding domain (ChtBD1; PF00187)

Boxed: Amino-acid change and the responsible SNP in the Vna-Va sequence alignment

Vna	ATGCGTTTCTCCGCGTTCTTACCCTCTGCTCGTGGCCTGCGCCGGCCAAACCTCAT	60
Va	ATGCGTTTCTCCGCGTTCTTACCCTCTGCTCGTGGCCTGCGCCGGCCAAACCTCAT *****	60
P_Vna	<u>MetArgPheSerAlaValLeuThrAlaLeuLeuValAlaCysAlaAlaAlaLysProHis</u>	20
Δ		20
Vna	GGCAAGCGTGACGTGTGCCCGCCAAGCCCCCAAGAGCAGCCAGTCGAGTACTGCAACA	120
Va	GGCAAGCGTGACGTGTGCCCGCCAAGCCCCCAAGAGCAGTCAGTCGAGCACTGCCACA *****	120
P_Vna	GlyLysArgAspValCysProAlaLysProProLysSerSerGlnSerSerThrAlaThr	40
Δ		40
Vna	ACTACTAGCAGTAGGCCAGCCCCGACTGGGCCCTTTTCCGACGACGCTCTTGC GGTTGGC	180
Va	ACTACTAGCAGTAGGCCAGCCCCGACTGGGCCCTTTTCCGACGACGCTCTTGC GGTTGGA *****	180
P_Vna	ThrThrSerSerArgProAlaProThrGlyProPheSerAsp AspAlaSerCysGlyGly	60
Δ		60
Vna	CCCAACAA C TTTGTCTGCGCTCTGGGACATGCTGCTCCAGTGCCA ACTTCTGCGGCGTC	240
Va	CCCAACAA A TTTCGTCTGCGCTCTGGGACATGCTGCTCTAGTGCCA ACTTCTGCGGCGTC *****	240
P_Vna	ProAsnAsnPheValCysArgSerGlyThrCysCysSerSerAlaAsnPheCysGlyVal	80
Δ	Arg	80
Vna	ACTGCTGCCACTGCGAGG C AGGCTGCC A ACCTG G ATTGGGTGATTGCGCTCTCAATTC	300
Va	ACTGCTGCCACTGCGAGG G AGGCTGCC G ACCTG A ATTGGGTGATTGCGCTCTCAATTC *****	300
P_Vna	ThrAlaAlaHisCysGluAlaGlyCysGlnProGlyLeuGlyAspCysGlySerGlnPhe	100
Δ	Thr Arg Glu	100
Vna	GTCAAAATCTCGACCGGGCCTCCTGGCAGTGTTCGACCGACGGTACCTGCGGCGGCACC	360
Va	GTCAAAATCTCGACCGGGCCTCCTGGCAGTGTTCGACCGACGGTACCTGCGGCGGCACC *****	360
P_Vna	ValLysIleSerThrGlyProProGlySerValSerThrAspGlyThrCysGlyGlyThr	120
Δ		120
Vna	AACGGCTGGATATGCCCCAAAGGCAACTGCTGCTCGGATTCCGGCTTCTGTGGTGCTACA	420
Va	AACGGCTGGATATGCCCCAAAGGCAACTGCTGCTCGGATTCCGGCTTCTGTGGTGCTACA *****	420
P_Vna	AsnGlyTrpIleCysProLysGlyAsnCysCysSerArgPheGlyPheCysGlyAlaThr	140
Δ		140
Vna	GCTGATCACTGCGCCCCGGCTGCCAGCCC G CCTTTGGTATCTGTCCAACCCACCCT	480
Va	GCTGATCACTGCGCCCCGGCTGCCAGCCC A CCTTTGGTATCTGTCCAACCCACCCT *****	480

P_Vna	AlaAspHisCysAlaProGlyCysGlnProAlaPheGlyIleCysProAsnProThrPro	160
Δ	Thr	160
Vna	GGCGTAATGCCTCGCCTGACGGCACTTGCGGTGGCTCTAACAAGTTTATCTGCGCTTCC	540
Va	GGCGTAATGCCTCGCCTGACGGCACTTGCGGTGGCTCTAACAAGTTTATCTGCGCTTCC *****	540
P_Vna	GlyGlyAsnAlaSerProAspGlyThrCysGlyGlySerAsnLysPheIleCysAlaSer	180
Δ		180
Vna	GGGACCTGCTGCTCCAAGGCTGGCTTCTGTGGTAACTACTAAGGACCACTGCGACGCCGGC	600
Va	GGGACCTGCTGCTCCAAGGCTGGCTTCTGTGGTAACTACTAAGGACCACTGCGACGCCGGC *****	600
P_Vna	GlyThrCysCysSerLysAlaGlyPheCysGlyAsnThrLysAspHisCysAspAlaGly	200
Δ	Thr	200
Vna	TGCCAGTTTGATTTTGGTAGCTGCGGCGACGCTTTCGTCCCGGTCCCGGGCGGTAATCCC	660
Va	TGCCAGTTTGATTTTGGTAGCTGCGGCGACGCTTTCGTCCCGGTCCCGGGCGGTAATCCC *****	660
P_Vna	CysGlnPheAspPheGlySerCysGlyAspAlaPheValProValProGlyGlyAsnPro	220
Δ		220
Vna	CCGCCCCGCGGTAGTGTCTCTACCGATGGCACCTGCGCTGGTGCTAACGGCTTGATCTGT	720
Va	CCGCCCCGCGGTAGTGTCTCTACCGATGGCACCTGCGCTGGTGCTAACGGCTTGATCTGT *****	720
P_Vna	ProProArgGlySerValSerThrAspGlyThrCysAlaGlyAlaAsnGlyLeuIleCys	240
Δ		240
Vna	CCTCAAGGCAACTGCTGCTCGCGATTTGGCTTCTGTGGTGCTACAGCTGATCACTGCGGC	780
Va	CCTCAAGGCAACTGCTGCTCGCGATTTGGCTTCTGTGGTGCTACAGCTGATCACTGCGGC *****	780
P_Vna	ProGlnGlyAsnCysCysSerArgPheGlyPheCysGlyAlaThrAlaAspHisCysGly	260
Δ		260
Vna	ACCGGCTGTGCTAGTTCAGCCTTCGGTATCTGTAACACCGCGGTGCCACATCTTCTTCGACC	840
Va	ACCGGCTGTGCTAGTTCAGCCTTCGGTATCTGTAACACCGCGGTGCCACATCTTCTTCGACC ****	840
P_Vna	ThrGlyCysGlnSerAlaPheGlyIleCysAsnThrGlyGlyAlaThrSerSerSerThr	280
Δ	Asp Pro	280
Vna	AGCTCGAAGCCGGCCCTACCGGCGGCATCTCGCCCGATGGCTCTTGCGGCGGCACCAAC	900
Va	AGCTCGAAGCCGGCCCTACCGGCGGCATCTCGCCCGATGGCTCTTGCGGCGGCACCAAC *****	900
P_Vna	SerSerLysProAlaProThrGlyGlyIleSerProAspGlySerCysGlyGlyThrAsn	300
Δ		300
Vna	GGCTTACCTGCACACCGGGTAACTGCTGCTCACAGTTCGGTCTGTGGTGCTACGACT	960
Va	GGTTATACCTGCACACCGGGTAACTGCTGCTCACAGTTCGGTCTGTGGTGCTACGACT ** * *****	960
P_Vna	GlyPheThrCysThrProGlyAsnCysCysSerGlnPheGlyPheCysGlyAlaThrThr	320
Δ	Tyr	320
Vna	GGCCACTGCGGCCTGGTTGCCAGTCCGCCTTCGGTATCTGTGGCACCGGAGGCCTGCG	1020
Va	GGCCACTGCGGCCTGGTTGTCACTCAGCCTTCGGTATCTGTGGCACCGGCGGTGCTACC	1020

```

*****
P_Vna GlyHisCysGlyThrGlyCysGlnSerAlaPheGlyIleCysGlyThrGlyGlyProAla 340
Δ AlaThr 340

Vna TCTTCGTCGACCAGCTCCTCGAAACCCGCTCCTACCGGCGGCATTTCACCTGATGGCTCT 1080
Va TCTTCGTCGACCAGCTCCTCGAAACCCGCTCCTACCGGCGGCATTTCACCTGATGGCTCT 1080
*****

P_Vna SerSerSerThrSerSerSerLysProAlaProThrGlyGlyValSerProAspGlySer 360
Δ Ile 360

Vna TCGCGCGGCACTAACGGTTATACCTGCACAACAGGCAACTGCTGCTCACAGTACGGCTTC 1140
Va TCGCGCGGCACTAACGGTTATACCTGCACAACAGGCAACTGCTGCTCACAGTATGGCTTC 1140
*****

P_Vna CysGlyGlyThrAsnGlyTyrThrCysThrThrGlyAsnCysCysSerGlnTyrGlyPhe 480
Δ 480

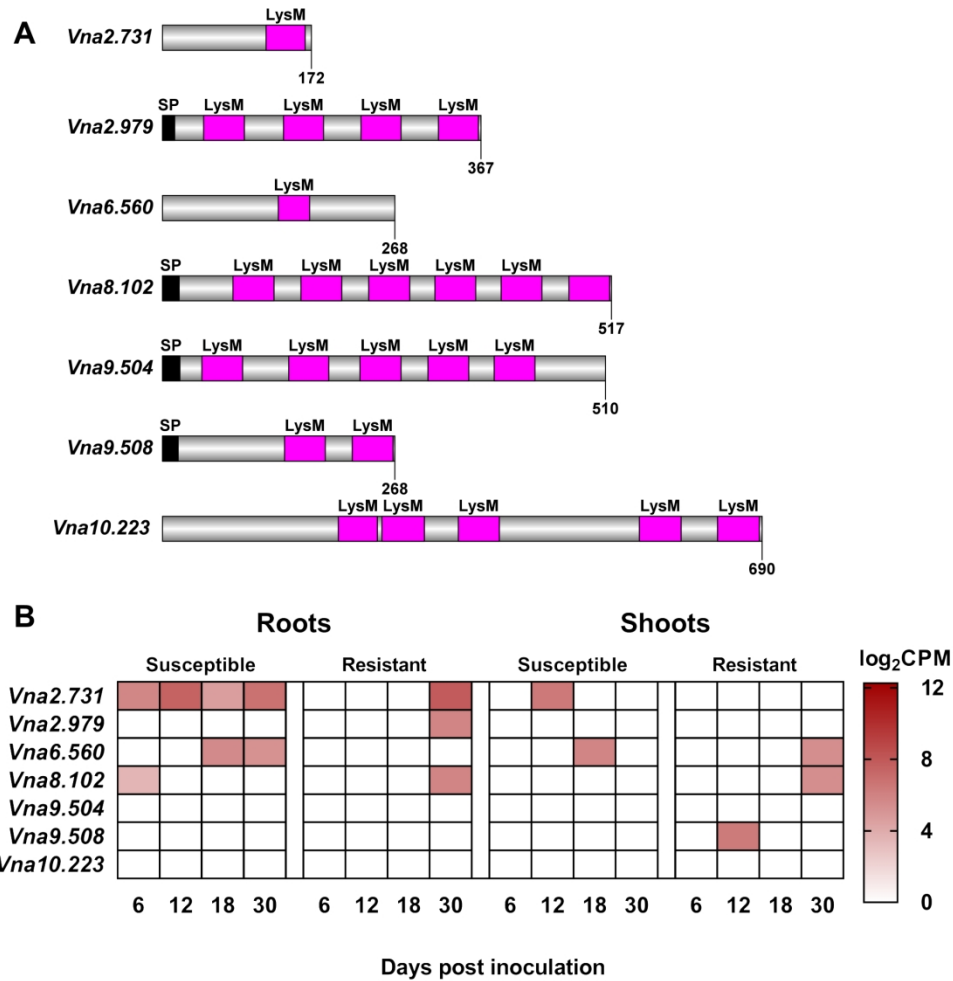
Vna TCGGGTGCCACGACTGGCCACTGCGGTACTGGCTGCCAGCGTGCCTTTGGTATCTGCACC 1200
Va TCGGGTGCCACGACTGGCCACTGCGGTACTGGCTGCCAGCGTGCCTTTGGTATCTGCACC 1200
*****

P_Vna CysGlyAlaThrThrGlyHisCysGlyThrGlyCysGlnArgAlaPheGlyIleCysThr 400
Δ Ala 400

Vna TAA 1203
Va TAA 1203
***

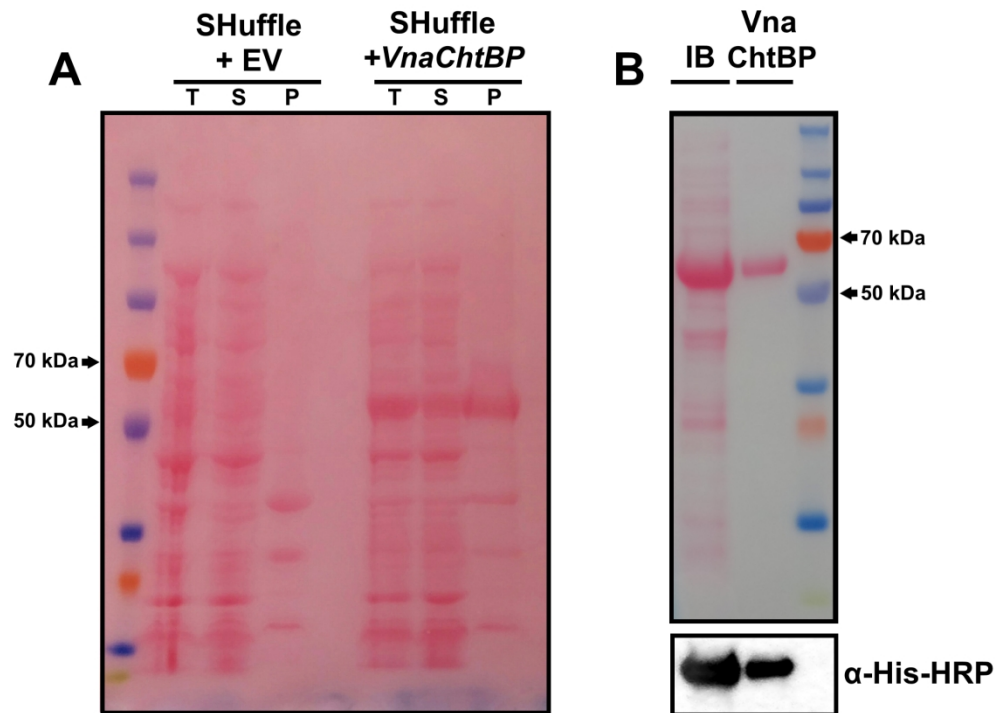
P_Vna stop
Δ

```



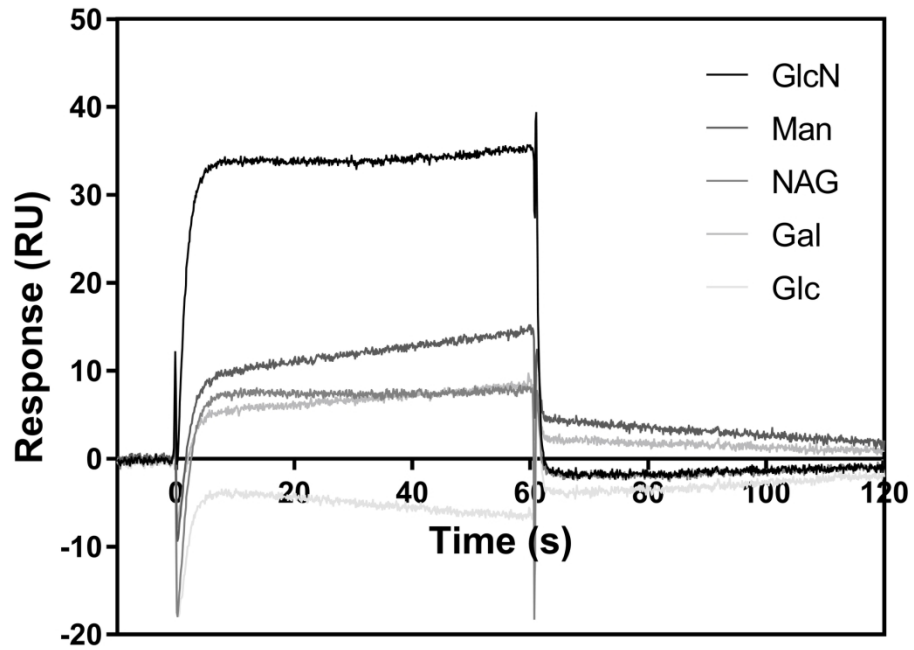
Domain architecture and gene expression of likely LysM effector proteins identified in *Verticillium nonalfalfae*. Protein organization was determined by matching protein sequences against the InterPro protein signature databases using the InterProScan tool. Results were presented by IBS software (Liu et al. 2015). Gene expression is presented as a heatmap of log₂CPM values determined by RNA sequencing of infected hop (Progar et al. 2017).

177x195mm (300 x 300 DPI)



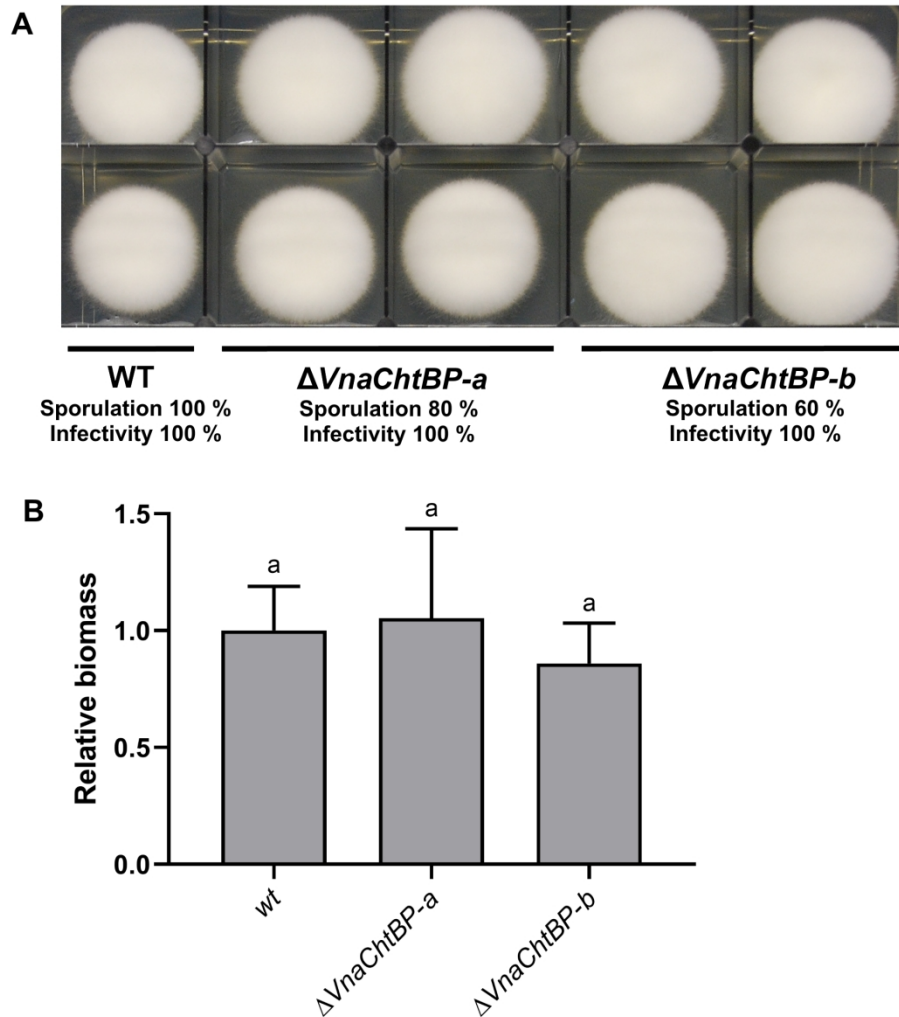
SDS-PAGE and western blot analysis of recombinant VnaChtBP production. Protein was expressed overnight at 16°C in *E. coli* SHuffle T7 cells (A), refolded from inclusion bodies (IB) using a mild solubilization method (Qi et al. 2015) and Ni-NTA affinity purified (B). Protein samples were separated by SDS-PAGE, transferred to a PVDF membrane and stained with Ponceau S. Western blot analysis was performed with primary antibody His-probe (H-3) (SCBT) (1:1,000) and secondary Chicken anti-mouse IgG-HRP (SCBT) (1:5,000). Protein bands were detected in the UVP gel imaging system using ECL substrate. T, total proteins; S, supernatant; P, pellet

177x169mm (300 x 300 DPI)



Binding of various carbohydrates to recombinant VnaChtBP. Protein (0.1 mg/ml) was immobilized to the surface of a CM5 sensor chip and binding of N-acetyl glucosamine (NAG), glucosamine (GlcN), glucose (Glc), galactose (Gal) and mannose (Man) at a 500 μ M concentration in HBS buffer (10 mM HEPES, 140 mM NaCl, pH 7.4) was monitored on Biacore T100.

177x122mm (300 x 300 DPI)



The morphology, sporulation and infectivity of *Verticillium nonalfalae* wild type and *VnaChtBP* knockout mutants (A) and relative fungal biomass quantification in infected hop (B). Sporulation assessment 5 denotes 100% conidiation, while 1 denotes 20% conidiation of the wild type. Infectivity of 100% means all plants were infected with *V. nonalfalae* as determined by fungal re-isolation from infected hop. The relative quantity of *V. nonalfalae* DNA in infected hop was estimated at 21 dpi with the $2^{-\Delta\Delta C_t}$ method (Schmittgen and Livak 2008) using *V. nonalfalae* lethal genotype (PG2) specific primer 5-1gs (Radišek et al. 2004) and hop reference gene *DRH1* (DEAD box RNA helicase) for normalization (Štajner et al. 2013). Amplification levels are expressed relative to those obtained from plants infected with the wild type strain. One-way ANOVA with Tukey's multiple comparison test was performed in GraphPad Prism 8.02 (GraphPad Software, San Diego, California USA, www.graphpad.com) to test for difference between the wild type and mutant group means.

177x193mm (300 x 300 DPI)